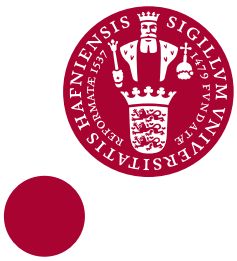

Relation between seasonally detrended shortwave infrared reflectance data and land surface moisture in semi-arid Sahel

Olsen, Jørgen Lundegaard; Ceccato, Pietro; Proud, Simon Richard; Fensholt, Rasmus; Grippa, Manuela; Mougin, Eric; Ardö, Jonas; Sandholt, Inge

Published in:
Remote Sensing

DOI:
10.3390/rs5062898

Publication date:
2013

Document version
Publisher's PDF, also known as Version of record

Remote Sens. **2013**, *5*, 2898-2927; doi:10.3390/rs5062898

OPEN ACCESS

Remote Sensing

ISSN 2072-4292

www.mdpi.com/journal/remotesensing

Article

Relation between Seasonally Detrended Shortwave Infrared Reflectance Data and Land Surface Moisture in Semi-Arid Sahel

Jørgen L. Olsen [1,*], Pietro Ceccato [2], Simon R. Proud [1], Rasmus Fensholt [1], Manuela Grippa [3], Eric Mougin [3], Jonas Ardö [4] and Inge Sandholt [1]

[1] Department of Geosciences and Natural Resource Management, University of Copenhagen, Øster Voldgade 10, DK-1350 Copenhagen K, Denmark; E-Mails: srp@geo.ku.dk (S.R.P.); rf@geo.ku.dk (R.F.); is@geo.ku.dk (I.S.)

[2] The International Research Institute, Columbia University, 61 Route 9W, Palisades, NY 10964, USA; E-Mail: pceccato@iri.columbia.edu

[3] Centre d'Etudes Spatiales de la BIOsphere (CESBIO), UMR 5126 UPS-CNRS-CNES-IRD, 18 Avenue Edouard Belin, bpi 2801, F-31401 Toulouse Cedex 9, France; E-Mails: Manuela.grippa@get.obs-mip.fr (M.G.); mougin@lmtg.obs.fr (E.M.)

[4] Department of Physical Geography and Ecosystems Science, Lund University, Sölvegatan 12, SE-22362 Lund, Sweden; E-Mail: jonas.ardo@nateko.lu.se

* Author to whom correspondence should be addressed; E-Mail: jlo@geo.ku.dk; Tel.: +45-353-22543 or +45-353-22500; Fax: +45-3532-2100.

Received: 18 April 2013; in revised form: 23 May 2013 / Accepted: 23 May 2013 / Published: 6 June 2013

Abstract: In the Sudano-Sahelian areas of Africa droughts can have serious impacts on natural resources, and therefore land surface moisture is an important factor. Insufficient conventional sites for monitoring land surface moisture make the use of Earth Observation data for this purpose a key issue. In this study we explored the potential of using reflectance data in the Red, Near Infrared (NIR), and Shortwave Infrared (SWIR) spectral regions for detecting short term variations in land surface moisture in the Sahel, by analyzing data from three test sites and observations from the geostationary Meteosat Second Generation (MSG) satellite. We focused on responses in surface reflectance to soil- and surface moisture for bare soil and early to mid- growing season. A method for implementing detrended time series of the Shortwave Infrared Water Stress Index (SIWSI) is examined for detecting variations in vegetation moisture status, and is compared to detrended time series of the Normalized Difference Vegetation Index (NDVI). It was found

that when plant available water is low, the SIWSI anomalies increase over time, while the NDVI anomalies decrease over time, but less systematically. Therefore SIWSI may carry important complementary information to NDVI in terms of vegetation water status, and can provide this information with the unique combination of temporal and spatial resolution from optical geostationary observations over Sahel. However, the relation between SIWSI anomalies and periods of water stress were not found to be sufficiently robust to be used for water stress detection.

Keywords: soil moisture; vegetation; water stress; Earth observation; MSG SEVIRI; SIWSI; NDVI; Sahel; drought

1. Introduction

Land surface moisture is an important environmental factor in the Sudano-Sahelian areas of Africa, as water is the primary restricting factor of vegetation growth [1] and droughts can therefore have serious impacts on natural resources and food production, with far ranging consequences for the population of the region. At the same time, land surface moisture is a significant component of the hydrologic cycle [2] with important feedback to the atmosphere [3]. Monitoring surface moisture to detect drought is a challenging subject, and due to a generally insufficient number of conventional ground based climate observation sites in the region, the development of reliable Early Warning Systems (EWS) exploiting the capabilities of Earth Observation (EO) data for this purpose, has been an important topic for decades [4–6].

Today a number of techniques for estimating surface moisture exist, each based on different parts of the electromagnetic spectrum or a combination thereof. Widely used techniques are based on microwave data, for instance the European SMOS sensor [7], others take advantage of the information in the thermal infrared bands, like those for instance reported in [8–11]. In addition, vegetation indices (VI) have been applied and analyzed in order to assess land surface moisture status. The potential of shortwave infrared (SWIR) data to produce estimates of vegetation water content has also been widely examined and applied, and much research has gone into the use of SWIR data acquired from multispectral and hyperspectral instruments onboard satellites and aircrafts, with published studies dating back to the 1960s [12–16]. Still, the ultimate indicator remains to be found, as all approaches have unresolved issues, examples being that microwave has either low temporal resolution or very coarse spatial resolution, thermal infrared primarily works when there is no or little vegetation, and SWIR only when there is close to full vegetation cover. Common to all the above mentioned data sources, are the influence of vegetation cover on the results. Likewise, the temporal resolution of the available data may not be adequate for studying changes in land surface moisture status, or the response time in the observed variable is too long. In this study, we explored the potential of SWIR wavebands for estimating land surface moisture in a semiarid environment in the Sahel. Two case studies were investigated in detail to estimate land surface moisture: (1) when the soil is bare and (2) when the soil is increasingly covered by vegetation during the growing season. Analyses are based on data from the Spinning Enhanced Visible and Infrared Imager (SEVIRI) sensor on board the

geostationary satellite Meteosat Second Generation (MSG) and *in situ* measurements from three test sites across the Sahel. Our objectives were to determine the potential of SWIR as a land surface moisture indicator during these two different stages, and to ascertain if periods of vegetation water stress can reliably be detected from time series of SWIR based indices.

2. Background

2.1. Thermal Infrared and Vegetation Indices

Thermal Infrared (TIR) information, combined with spectral VIs, has been used for numerous investigations into remote sensing based estimations of soil moisture, drought, and plant water stress [8–10,17–19]. The combination of a vegetation index and TIR has been used to provide indirect information on surface moisture and evapotranspiration, as daytime temperatures in semi-arid areas such as the Sahel increase quickly when a surface dries. The most commonly used VI is the Normalized Difference Vegetation Index (NDVI) [20], which can be related to important vegetation parameters, such as fractional vegetation cover, through simple but not necessarily linear transformation. NDVI has also been found sensitive to Leaf Area Index (LAI), but this sensitivity may be viewed as sensitivity to the bare soil component when LAI is between 2 and 4 or below [21]. One method for interpretation of Ts/NDVI scatter plots uses isolines to estimate water availability for evapotranspiration, and has been widely applied and is well described in [10]. Further developing this idea, Krapez *et al*. [11] proposed adding an extra dimension to the triangle method, turning the 2D plot into a 3D representation, by adding either albedo or the Cellulose Absorption Index (CAI) [22] as a third variable, and thereby increasing the correlation between the calculated and measured moisture.

2.2. Shortwave Infrared Data for Moisture Assessment

For green vegetation the reflectance in the SWIR (1.3–2.5 μm) spectral region is largely controlled by the quantity of liquid water present in the leaf biomass of the canopy, due to the strong absorption by water in this spectrum [23], often expressed as Equivalent Water Thickness (EWT). With focus on applicability for satellite remote sensing, a study of the SWIR spectrum was carried out by [14], concluding that the 1.55–1.75 μm wavelength interval was the best suited for observing plant canopy water status, when taking into account both atmospheric transmission and incident solar radiation. Other studies have found various advantages in using the SWIR spectral region for soil and vegetation moisture studies. A well documented effect of moisture is to darken soils (review in [24]) and in a study of cotton canopies with various soil backgrounds by [25] it was found that soil type and soil brightness have a large influence on the reflectance measured in the red and NIR spectrums for a mixed pixel, with less than ~75% vegetation cover. Using laboratory spectroscopy [26] showed that variations in reflectance induced by different soil types were smaller for the SWIR spectrum than for the visible and near infrared (VNIR) spectrum, reducing uncertainty due to variation in soil properties when relating moisture and reflectance. They also demonstrated a greater sensitivity at high soil moisture content for SWIR wavelengths, as the VNIR signal saturated when volumetric water content exceeded 20%, whereas SWIR remained sensitive up to a volumetric water content of 50%. Also using laboratory spectroscopy, on soil samples of various textures collected in the Ganges and Brahmaputra

river systems, Small *et al*. [27] measured the increase in short wave reflectance as samples were drying. It was concluded that the consistency of spectral variation with moisture content has encouraging implications for soil moisture mapping, using high spatial resolution broadband satellite instruments or hyperspectral instruments like HyMap and Airborne Visible/Infrared Imaging Spectrometer (AVIRIS). The laboratory spectroscopy data of soil and moisture from different studies are consistent with findings based on albedo field estimates and a MODIS albedo product reported in [28], who identified rainfall as having a large influence on short term albedo variations on bare soils in the Sahel, while during the rainy season plant growth caused the largest changes in albedo.

2.3. Vegetation Water Sensitive Indices

The SWIR spectrum is not only sensitive to liquid water content of the canopy, but also to leaf internal structure and leaf dry matter content. This can be minimized by combining SWIR spectrum data with data from the NIR spectrum, as the NIR is only sensitive to leaf internal structure and leaf dry matter content [29]. Several such vegetation moisture sensitive indices based on combinations of NIR and SWIR information have been suggested; among these are the Normalized Difference Water Index (NDWI) using spectral reflectance measurements centered around the 0.86 μm and 1.24 μm wavelengths [16], the Global Vegetation Moisture Index (GVMI) based on the 0.45 μm blue to rectify the NIR for atmospheric perturbations, 0.82 μm NIR, the 1.6 μm SWIR reflectance bands of SPOT VGT [30,31], and the Shortwave Infrared Water Stress Index (SIWSI) derived from the Moderate Resolution Imaging Spectroradiometer (MODIS) NIR 0.86 μm and SWIR 1.6 μm bands [32]. The SIWSI (Equation (1)) has been found to be sensitive to leaf water content and has shown a strong correlation to surface moisture estimates in the Sahel:

$$SIWSI = (\rho SWIR - \rho NIR) / (\rho SWIR + \rho NIR) \quad (1)$$

where ρ is reflectance for the SWIR and NIR bands.

SIWSI was designed to utilize MODIS bands 2 (0.86 μm NIR) and 6 (1.6 μm SWIR), as it was determined that the 1.6 μm SWIR is more sensitive to leaf water content than band 5 (1.2 μm) in northern Senegal [32]. The NDWI on the other hand makes use of the 0.86 μm and 1.2 μm SWIR. It has been found that while 1.6 μm is more sensitive to water content it also saturates sooner with increasing vegetation cover, at LAI around four or five, whereas the 1.2 μm SWIR spectrum, despite being less sensitive, only saturates with LAI around eight [16]. The LAI in the Sahel rarely exceeds three, so the additional range of the 1.2 μm wavelength before saturation occurs is not needed. For a sample of species in northern Italy it has been found that SWIR sensitivity to EWT decreases as EWT increases [29] further indicating the saturation of NIR/SWIR vegetation water indices for dense canopies. The SIWSI has been reported to perform less well for surfaces with less than full vegetation cover, such as in the early growing season in a semi-arid area [32,33]. Likewise it is difficult to infer EWT from NDWI under less than full vegetation cover [16], and a LAI lower than two has been found problematic for the GVMI as the soil background influences the index [30].

It has been noticed that SIWSI, for a semi-arid location, follows NDVI very closely, as both are primarily dependent on plant phenology [34]. In order to extract information on non-phenology dependent variations in water status, the phenology needs to be taken into account. This has previously been done by applying SIWSI when full vegetation cover is reached, and before senescence, when

changes observed could therefore be attributed to changes in vegetation water status [32,34]. In this study we investigate further the relationship between SIWSI and vegetation water content by studying the growing period of vegetation from the beginning of the growing season to senescence.

Recent use of MSG SEVIRI channel 2 (NIR 0.8 μm) and 3 (SWIR 1.6 μm) data to implement the SIWSI showed the advantage of utilizing the high temporal resolution of instruments mounted on geostationary platforms, as the SEVIRI SIWSI was observed not just to follow the phenology, but also to covary with short term changes of *in situ* measured moisture indicators once full vegetation cover was reached [34]. In contrast, covariation of short term changes was not observed between MODIS SIWSI and *in situ* measured moisture indicators for the same time period.

3. Study Sites

Data from three test sites situated across the semi-arid Sahel have been used in this study: Dahra, Agoufou, and Demokeya. Information on site characteristics summarized here (Table 1) is previously published in the references noted for each site. The years 2006 and 2008–2010 are used from Dahra, the years 2007 and 2008 are used from Agoufou, and the years 2007–2009 are used from Demokeya. All three sites have one yearly rainy season, with majority of rainfall occurring in late July to September, initiating germination of annual species and the growing season onset. Average annual precipitation calculated from the Climate Prediction Center Rainfall Estimation product version 2.0 (CPC RFE2) over the period of 2001 to 2012 is shown in Figure 1 [35], and the average annual rainfall amount is relatively close for the three sites (Table 1 and Figure 1), but all sites have large variations both inter-annual and intra-seasonal. The soils are all sandy and have been classified as Arenosols according to the FAO reference base [36,37]. Negligible amounts of organic matter have been reported from all three sites.

Figure 1. Locations of test sites (black stars) in semi-arid Sahel and average annual rainfall from 2001 to 2012 calculated from CPC RFE v2 is shown in 200 mm intervals.

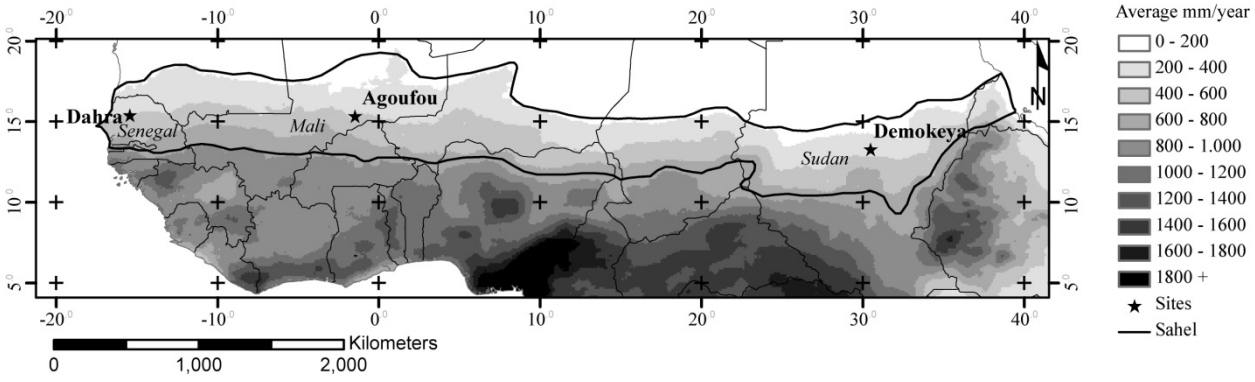

3.1. Dahra

The Dahra test site [38,39] is located in the Ferlo region in northern Senegal (Figure 1), with annual rainfall typically in the range of 300–600 mm. The location is relatively homogeneous in terms of soil, vegetation, and elevation and therefore well suited for comparison with mid- to low-spatial resolution Earth observation data. The herbaceous layer is dominated by annual grasses of the Poceae family such

as *Dactyloctenium aegypticum*, *Aristida mutabilis*, *Eragrostis tremula* and *Cenchrus bifloures*, as well as the legume *Zornia latifolia* (Fabaceae), and interspersed with few perennial grasses. Some year to year variations in plant species composition has been observed for the herbaceous layer. The woody vegetation consists of tree and shrub species, predominantly *Acacia tortilis, Acacia senegal,* and *Balanites aegyptiaca*. The tree canopy cover (TCC) does not exceed 5% [40] and the density of woody plants per area is relatively homogeneous. Biomass production of the herbaceous layer is sampled at this site, and it has been fenced off to avoid grazing. In December 2008 the area caught fire.

3.2. Agoufou

The Agoufou test site is part of the meso-scale Gourma observatory in Mali [41]. Gourma is the northern-most of three meso-scale sites deployed in West Africa as part of the African Monsoon Multi-Disciplinary Analysis (AMMA). Data from AMMA has been crucial in this study and we would like to acknowledge the contribution. Based on a French initiative, AMMA was built by an international scientific group and is currently funded by a large number of agencies, especially from France, UK, US and Africa. It has been the beneficiary of a major financial contribution from the European Community's Sixth Framework Research Programme [42]. Annual precipitation is in the range of 200–600 mm and the vegetation consists of an herbaceous layer and scattered trees and shrubs. The herbaceous layer is composed mainly of annual plants which are dominated by grasses of the Poaceae family, such as *Cenchrus biflorus*, *Aristida Mutabilis* and *Tragus berteronianus*, as well as the legume *Zornia glochidiata* of the Fabaceae family. Scattered bushes, shrubs and low trees only constitute about 3% of the canopy. The dominant woody species are *Acacia raddiana, Combretum glutinosum, Balanites aegyptiaca, Acacia Senegal,* and *Leptadenia pyrotechnica*. The site is situated in a landscape of gently undulating fixed sandy dunes with a higher density of woody plants in depressions between dunes [43]. The wilting point and field capacity is comparable to Dahra (Table 1, [38,44]).

Table 1. Rainfall, soil and vegetation characteristics as published in the noted references, where more extensive descriptions of the sites can also be found.

	Dahra, Senegal [38,44]	**Agoufou, Mali [41]**	**Demokeya, Sudan [45,46]**
Latitude/longitude	15.40°N; 15.43°W	15.35°N; 1.48°W	13.28°N; 30.48°E
Wet season	July–October	June–September	July–October
Average annual rainfall	360 mm	375 mm	320 mm
Soil type	Luvic Arenosols	Arenosols (fixed dunes)	Cambic Arenosols
Soil texture (% clay/silt/sand)	0.4/4.6/95	4.6/3.3/90	0/3.5/96.5
Field capacity, FC (vol.%)	6.9	7	15
Wilting point, WP (vol.%)	2.8	2.5	5
Vegetation type	Open woody savanna	Open woody savanna	Sparse savanna grassland/ Open woody savanna

3.3. Demokeya

The Demokeya test site [45,46] is named after the nearby village and is located in the Kordofan region in Sudan, 35 km north-east of El Obeid, between the 300 and 400 mm isohyets. The herbaceous

layer is dominated by annual and perennial grasses including the annuals *Eragrostis tremula, Cenchrus biflorus* and some herbs, and the perennial *Aristida pallida*. The dominating woody species are of the *Acacia* genus, including *Acacia nilotica, Acacia tortilis,* and *Acacia Senegal* and constitute 5%–10% of canopy cover. The soil is sandy (96.5% sand) and reported to have wilting point and field capacity at respectively 0.05 and 0.15 $m^3 \cdot m^{-3}$ (equaling 5 vol.% and 15 vol.%).

4. Data

4.1. Meteosat Second Generation (MSG) Spinning Enhanced Visible and InfraRed Imager (SEVIRI)

The SEVIRI instrument onboard the MSG geostationary platform provides observations every 15 min from its location at 0° longitude over the equator. The observations produced are at 10 bits radiometric resolution and a 3 km sampling resolution at sub satellite point in 12 spectral channels, including a high resolution broadband visible channel with a 1 km spatial sampling distance [47]. Level 1.5 MSG SEVIRI data are acquired in real time through the EUMETCast service, and an operational MSG SEVIRI processor has been built at the Department of Geosciences and Natural Resource Management, University of Copenhagen [39] to compute Earth surface reflectances. Atmospheric correction was performed using an improved version [48] of the SMAC algorithm [49] using daily values of atmospheric water vapor, ozone and aerosols from the Level-3 MODIS Terra and Aqua Atmosphere Daily Global Products as inputs. All MSG SEVIRI data are cloud-masked using the EUMETSAT CMa [50].

The atmospherically corrected and cloud masked Earth land surface reflectances from SEVIRI are affected by the changing illumination and viewing geometry between sun, target, and sensor. This can be minimized by using a Bidirectional Reflectance Distribution Function (BRDF) to describe the angular dependency, making it possible to produce reflectances normalized to a common set of solar and viewing angles. A Nadir view BRDF Adjusted Reflectance (NBAR) product has been created on a daily basis for channel 1 (VIS 0.6 μm), channel 2 (NIR 0.8 μm), and channel 3 (SWIR 1.6 μm), by using a modified version of the algorithm used for the MODIS Nadir BRDF-Adjusted Reflectance (NBAR) product [51,52]. The NBAR product is created as a rolling average using four days of observations as input (the given day and the three previous days). The product is sensitive to short term variations of surface reflectance, while the chance of retrieving sufficient cloud free observations for a successful inversion greatly increases by combining several days of data [52].

4.2. In situ *Measurements*

Multiple years of growing season time series with measurements of near surface soil moisture and soil texture are used from all three sites. Additionally, measurements of radiometric, vegetation, and meteorological parameters have been conducted at the Dahra test site during growing seasons from 2001 to present, and will be used for more detailed analysis. Some change of parameters recorded has occurred due to upgrade or repair of equipment. Data from 2006, 2008, 2009, and 2010 have been used in this study as important field estimates of biomass were available for these years. Above-ground equipment was installed on a 13 m high aluminum mast. Rainfall was measured using two tip bucket gauges placed at 2 m height. The red and NIR reflectances were measured over grass cover from 12 m

height by Skye Instruments four-channel sensors (SKR 1850 series), and for this study we used measurements from between 9:00 am and 17:00 pm. In 2008, surface temperatures were also acquired over grass cover from 12 m height. These measurements would ideally be supplemented with SWIR measurements, but equipment for long term fully automatic acquisition in this spectrum was not available. Soil Moisture Content (SMC) in vol.% was measured using soil moisture sensors at 5 cm depth; although in 2006 SMC was measured at 10 cm depth. Soil temperature was also taken at 5 cm depth. SMC and soil temperature were both taken in close proximity of the main mast. All measurements were acquired at 15 min interval. A subset of data from 2006 and 2008 were used in order to analyze conditions in detail during bare soil, and provided two short time series: One in July 2006 and one in June/July 2008. Difference in scale is always an issue between satellite data and *in situ* data, especially with the coarse spatial resolution of MSG SEVIRI (3 km pixel size). For Dahra and Demokeya, no studies of the scale differences exist, but SMC measurements at Agoufou have been shown to be compatible with kilometric scale data [53].

Biomass data were collected at the Dahra test site using a destructive sampling method. Sampling was performed on 5 to 6 different dates during each growing season, with one sampling taken as close as possible to the period of peak biomass. The sampling technique is a two-level stratified random sampling design, meaning that two transects of the same length, crossing each other at the middle, are used as the stratification [54]. A similar technique was previously applied in the Sahel [55]. Sampling was performed along the same transects for each sampling date. The sampling transects are diagonals in a square area with sides measuring 500 meters. The size of the area that is transected by sampling lines provides a good basis for comparison with moderate to coarse resolution satellite data. So far data have been successfully gathered for four years: 2006, 2008, 2009, 2010 (Table 2). At each sampling date, biomass was harvested and root depth manually estimated at 28 locations of one square meter in size, 14 at each transect. After harvesting, the samples were weighed, and then dried for 24 h, after which they were weighed again, producing both fresh and dry biomass. The difference is a good estimate of the vegetation water content expressed in $g \cdot m^{-2}$. The root depth varied from under 5 cm in early growing season to 10–15 cm at growing season peak.

Table 2. Overview of Dahra biomass sampling.

Year	Number of Sampling Dates	First Sampling	Peak Sampling	Fresh Biomass at Peak Date (g/m^2)
2006	5	10 August	29 September	583
2008	6	1 August	27 September	1,056
2009	5	15 August	16 September	719
2010	6	7 August	18 October	1,238

5. Methods

We investigated the sensitivity of red, NIR and SWIR reflectance data to variations in surface moisture during the critical period from first rain, when conditions of bare soil and litter are still observed, to early and mid-growing season when full vegetation cover is present. This is the period which typically causes difficulties when implementing NIR-SWIR based indices for semi-arid regions. Red, NIR, and SWIR data from the time periods of available soil moisture measurements were extracted from the SEVIRI NBAR product for all three test sites, but *in situ* measurements of red and NIR were

only available from the Dahra test site. Unfortunately no *in situ* measurements are yet available in the SWIR spectrum from any of the test sites. The majority of our analysis was based on the extensive data set from the Dahra test site. *In situ* soil moisture measurements and SEVIRI red/NIR/SWIR data from both Agoufou and Demokeya were used to compare with the findings from the Dahra site, in order to assess the validity of our findings in a broader geographical context across the Sahel.

5.1. Examining Pre-Growing Season Periods

To analyze the effects of rainfall during conditions of bare soil and litter we examined the relationship between rainfall, near surface soil moisture, red and NIR reflectance, land surface temperature, and near surface soil temperature using *in situ* data from the Dahra test site for the pre-growing seasons of 2006 and 2008. The diurnal variation in reflectance can be affected by clouds, so to obtain reliable estimates of *in situ* reflectance during morning, midday, and afternoon for both dry and wet conditions, average values were calculated from one hour of observations (four consecutive observations). This was used to quantify the reduction in red and NIR reflectances after rainfall, while none or very little green vegetation is present. Furthermore, to compare the effect of rainfall on spectral reflectances with the effect of rainfall on normalized indices, daily averaged NDVI from between 10:00 and 16:00 were calculated using the same red and NIR *in situ* reflectance measurements. When examining the effect of variations in soil moisture, we also made comparison with *in situ* measurements of land surface temperature and soil temperature at 5 cm depth.

5.2. Detrending Indices during Vegetation Growth

The total amount of canopy water at any given time during a growing season is closely linked to phenology through biomass production, and as the SWIR part of the SIWSI index is very sensitive to canopy water content, phenology has a large influence on the index. The strong influence of phenology on SWIR reflectance makes it challenging to use this spectrum to observe short term changes in surface water status on, e.g., a sub-weekly time scale as an indicator of water stress in the vegetation, as the influence of overall seasonal phenology will be stronger than the influence of short periods of limited plant available water. To remove the influence of phenology from the SIWSI signal we investigated the potential of detrending time series of SIWSI calculated from SEVIRI NBARs. The anomalies of the detrended SIWSI time series were hypothesized to contain information on surface water status independent of phenology, as SWIR reflectance should decrease more slowly, compared to the overall trend, when little or no water is available for plant growth, thereby making a SIWSI time series deviate from the trend and resulting in increasing anomalies. Although NDVI is only indirectly sensitive to water status, it was also calculated on a daily basis from the SEVIRI NBARs, and time series were detrended in the same fashion as SIWSI for comparison. The overall trends of both SIWSI and NDVI growing season time series were described using two different fitting types: 2nd order polynomials and Savitsky-Golay filtering, the latter with windows of 30 days for SIWSI and 35 days for NDVI. The 2nd order polynomial provides simple and smooth fitting with no asymmetry, while the Savitsky-Golay fitting follows the times series more closely, providing two differently derived sets of anomalies for interpretation. When detrending time series cover an entire growing season, the start and end dates are also important and the selection of these can bias the anomalies noticeably, especially for

early growing season. For the growing seasons used in this study the starting day was selected as the first set of observations where a decrease in SIWSI of 0.05 or increase in NDVI of 0.05 was observed and lasted more than two days. This was done for each index individually, as they were not expected to decrease/increase simultaneously, although this often turned out to be the case. To assess the sensitivity of the SIWSI and NDVI anomalies to changes in surface water status, the anomalies were compared with near surface SMC (vol.%) at the three sites. At the Dahra site in 2006 the SMC was measured at 10 cm depth, while for all other years and all three sites it was measured at 5 cm depth. Of most interest are the variations in anomalies when low SMC, and thereby low water availability for plants, was observed for extended periods. At Dahra the average herbaceous root depth, estimated during biomass harvesting, was at most 15 cm, and comparison of anomalies with SMC measurements from a single depth was therefore feasible. At the Demokeya site [45] reported the majority of roots to be found at around 15 cm depths, but with some roots reaching as deep as ~1 m. For the Agoufou site, the root zone is likewise assumed to be the top 1 m [41,53,56]. The root depths can be taken into consideration if enough rainfall occurs to make SMC at larger depths increase.

6. Results

6.1. Land Surface Moisture during Period of Bare Soil

Dahra *in situ* data from the pre-growing season periods of bare soil reflectances in 2006 and 2008 are shown in Figure 2. The rainfall events during the 2006 bare soil period (Figure 2(A)) all occur between late afternoon and early morning. The smaller rainfall events on DOY 197 and 203 have very limited impact on the soil moisture at 10 cm depth, but still appears to initiate germination and greening with NDVI increasing steadily from DOY 199, whereas the 16 mm rainfall on DOY 202 causes an increase in soil moisture to 18 vol.%. Following, the soil moisture decreases to 12 vol.% during the first 3 hours and to 9 vol.% after 24 h. This rapid drain off is due to the sandy properties of the soil, also reflected in the low field capacity (Table 1). After the initial steep decrease, the soil moisture decreases by less than 1 vol.% per day. During the 2008 period of bare soil (Figure 2(B)) three rainfall events (total of 29 mm) were registered; DOY 182, 183 and 184, with the first two being only hours apart. As in 2006, the rainfall occurred between late afternoon and early morning, and the SMC followed the same pattern as in 2006, with a sharp increase followed by rapid draining. After ~24 h the SMC reaches around 8 vol.%–9 vol.%, after which the SMC decrease slows down. The one-hour averaged reflectances for mornings, middays and afternoons on days with night or morning rainfall events (wet days) were lower than on days without preceding rainfall (dry days), with the difference in percent between average reflectance for dry days and average reflectance for wet days being largest on mornings immediately after the rainfall (Tables 3 and 4). The difference in midday reflectance was not large for 2006, but a noticeable difference in midday reflectance between dry and wet days was observed in 2008. The daily averaged NDVI values calculated from *in situ* observations of bare soil conditions is unchanged immediately after rainfall on DOY 197 and 198 in 2006, and DOY 183 in 2008, but are observed to increase from DOY 199 and onwards in 2006, as plant germination and greening initiates. The number of days with reflectance measurements available from bare soil conditions, with variations in soil moisture, was however limited. As shown in Figure 2(B) the difference in surface temperature for the two dry and two wet days in 2008 was noticeable, especially in

terms of diurnal temperature range. This changes from 28 °C and 30 °C for DOY 181 and 182 respectively, to 15 °C and 10 °C for DOY 183 and 184, while the diurnal range in soil temperature at 5 cm depth is 10 °C and 12 °C for DOY 181 and 182, and reduced to 7 °C and 5 °C on DOY 183 and 184.

Figure 2. (**A**) Bare soil *in situ* data from Dahra test site, 2006. Rainfall events are shown together with Soil Moisture Content (SMC) (vol.%) at 10 cm depth, Red (red line) and Near Infrared (NIR) (green line) reflectance from 9:00 to 17:00; (**B**) Bare soil *in situ* data from Dahra test site, 2008. Rainfall events are shown together with SMC (vol.%) at 10 cm depth, Red (red line) and NIR (green line) reflectance from 9:00 to 17:00. In addition to Figure 2(A) land surface and soil temperatures are also shown.

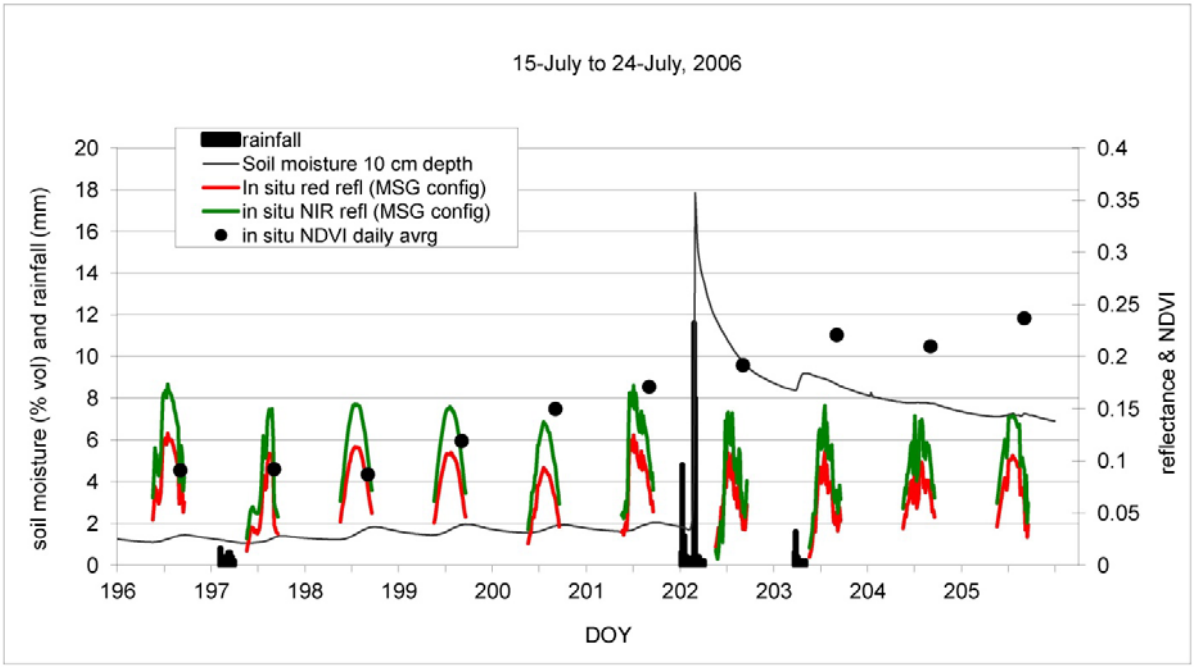

(**A**)

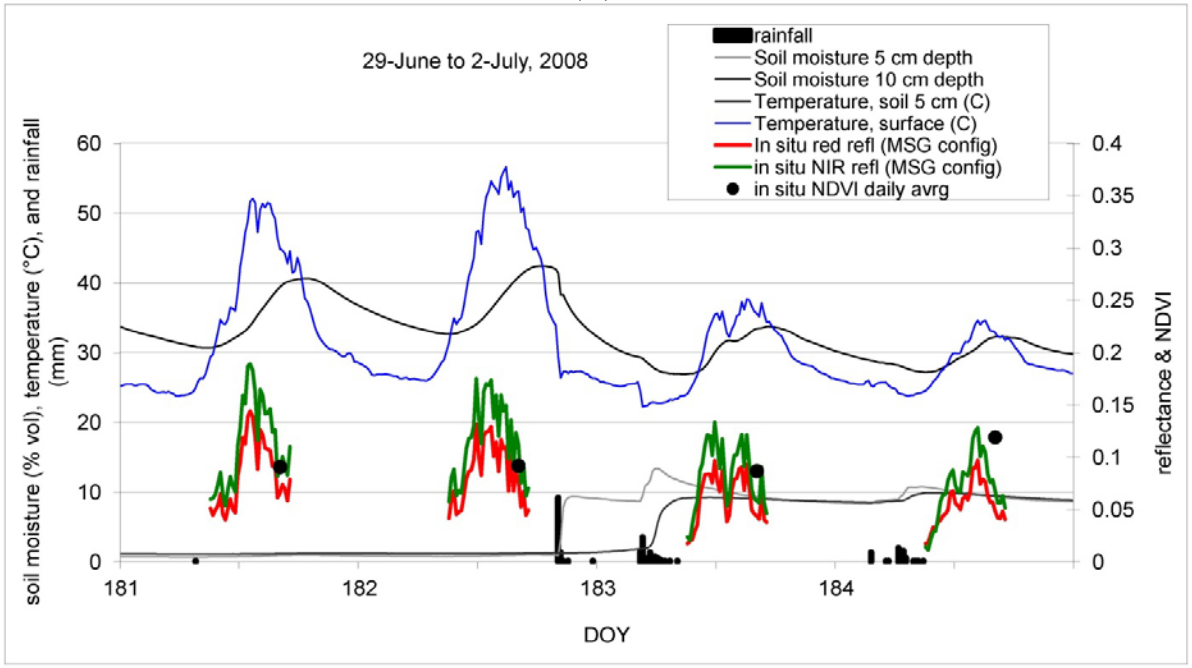

(**B**)

Table 3. Time of day specific averages of Red and Near Infrared (NIR) reflectance for dry and wet days respectively during the 2006 bare soil period.

Average Reflectance	Dry Days		Wet Days		Difference (%)	
	Red	NIR	Red	NIR	Red	NIR
Morning 9–10	0.047	0.071	0.022	0.028	53.0	61.4
Midday 12–13	0.102	0.143	0.078	0.110	23.6	22.9
Afternoon 16–17	0.057	0.082	0.040	0.058	29.5	29.0

Table 4. Time of day specific averages of Red and Near Infrared (NIR) reflectance for dry and wet days respectively during the 2008 bare soil period.

Average Reflectance	Dry Days		Wet Days		Difference (%)	
	Red	NIR	Red	NIR	Red	NIR
Morning 9–10	0.082	0.070	0.025	0.029	69.3	58.4
Midday 12–13	0.116	0.157	0.062	0.084	46.7	46.7
Afternoon 16–17	0.064	0.089	0.045	0.060	29.4	32.0

The short term changes in red and NIR reflectances, caused by rainfall events during the two periods of bare soil (Figure 2), are congruent with the short term albedo variability caused by rainfall outside of the growing season in the Sahel, as reported by [28]. The limited time period during which the rainfall induced reflectance changes were observable can be explained by a combination of several factors: (i) timing and quantity of rainfall, (ii) sandy properties of the soil, (iii) high temperatures causing high evaporation rates, and (iv) lack of vegetation. The additional hours of reduced bare soil reflectance observed during the 2008 bare soil case period, as compared to 2006, can be explained by timing and quantity of rainfall. The 2008 precipitation occurred closer to the 9 am morning reflectance measurements, allowing additional hours of measurements where reflectance was noticeable affected. The response in observed surface and soil temperatures in 2008 following the rainfall is very clear with the presence of water decreasing the diurnal temperature range for both surface and soil.

6.2. Land Surface Moisture during Period of Vegetation Growth

Four years of detailed observations covering full growing seasons from Dahra (2006, 2008, 2009, and 2010), are shown in Figure 3 with *in situ* measurements, SEVIRI SIWSI and SEVIRI NDVI. Large inter-annual variations were observed in the growing season onset, length and rainfall quantity and distribution. When comparing the relatively smooth curves of *in situ* NDVI time series with the NDVI time series calculated from SEVIRI NBAR product (Figure 3), it highlights the SEVIRI NDVIs overall lower values and larger noise content. The SEVIRI SIWSI time series appears less noisy as compared to SEVIRI NDVI. This can be due to atmospheric influences, which are larger for shorter wavelengths, as utilized by, e.g., [30,57,58]. Note that the low NDVI in 2009 despite abundant water can be a carryover effect from the fire in late 2008.

Figure 3. Dahra growing seasons of (**A**) 2006, (**B**) 2008, (**C**) 2009, and (**D**) 2010. For the first three years rainfall is shown, and for all four years soil moisture in vol.% at 5 or 10 cm depth is shown. Both *in situ* Normalized Difference Vegetation Index (NDVI) and Spinning Enhanced Visible and Infrared Imager (SEVIRI) NDVI are shown together with SEVIRI Shortwave Infrared Water Stress Index (SIWSI).

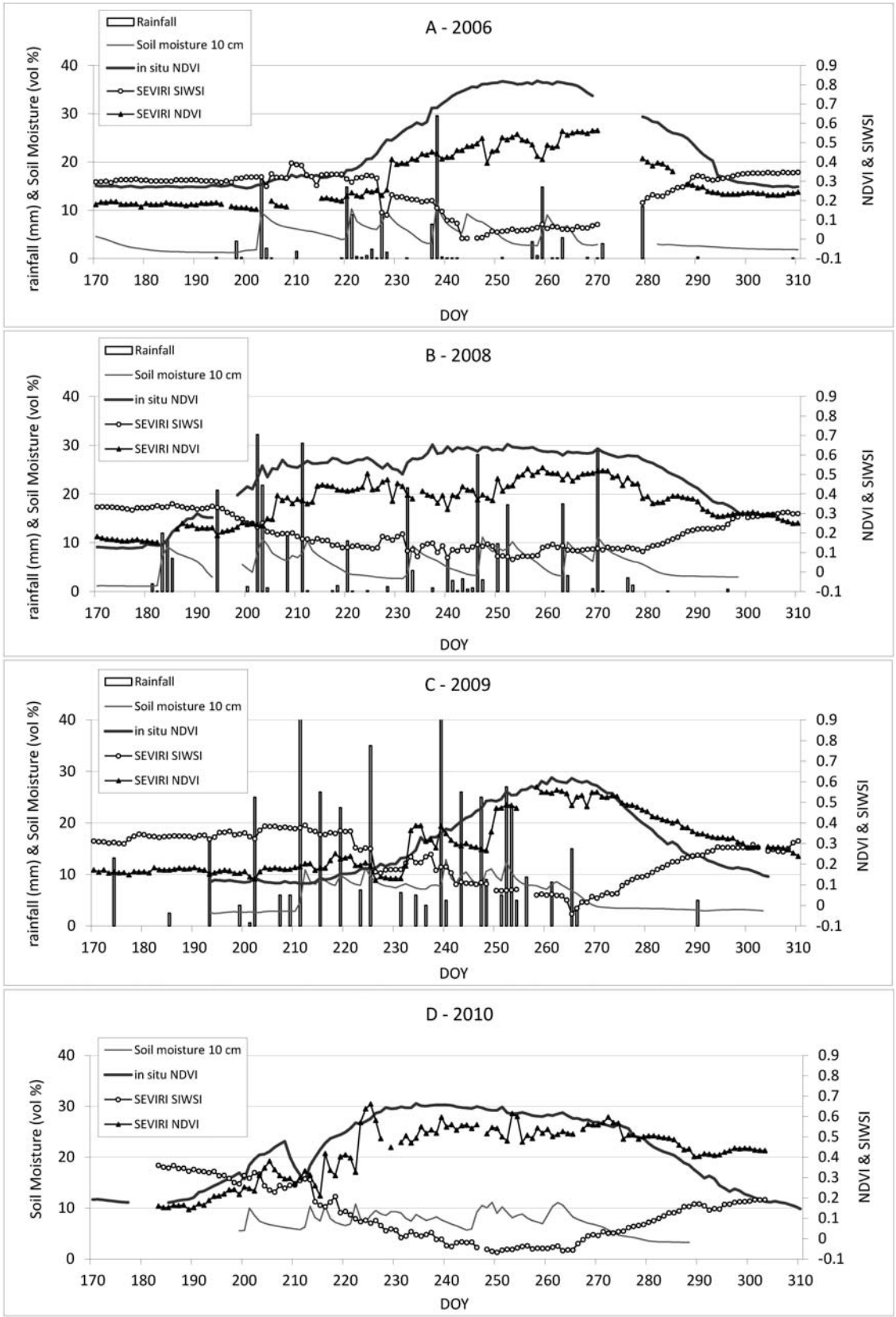

In Figure 4, time series of SEVIRI SIWSI and SEVIRI NDVI growing seasons are shown for all sites together with *in situ* measurements of fresh biomass and vegetation water content from Dahra (Figure 4(A–D)). Second order polynomials and Savitsky-Golay filter for detrending are fitted to the SIWSI and NDVI growing season curves. At Dahra in 2006 and 2009 the water content at peak biomass is approximately the same, although 2009 has more biomass. The SIWSI trend indicates an overall similar curve with comparable minimum values at mid-growing season for these two years. The 2008 growing season was longer (Figure 3) and with higher water content and biomass, but SIWSI values were higher than for any of the other years (Figure 4(B)). By comparing satellite and *in situ* data it was determined that the high SIWSI values were due to unexpected low NIR reflectance. At Dahra, out of the four years examined, 2010 had the highest water content, the most biomass, and the lowest overall SIWSI values. The 2010 growing season was shorter than 2008, but longer than 2006 and 2009.

Figure 4. Times series of satellite based Shortwave Infrared Water Stress Index (SIWSI) and Normalized Difference Vegetation Index (NDVI) extracted from the pixels overlapping test sites, including growing season trends described by 2nd order polynomials and Savitsky-Golay smoothing functions, for both SIWSI and NDVI. (**A–D**) show Dahra. (**E**,**F**) show Agoufou. (**G–I**) show Demokeya. X-axis shows Day of Year. Black lines: Spinning Enhanced Visible and Infrared Imager (SEVIRI) SIWSI, dashed black lines: SIWSI 2nd order trend, dotted black lines: SIWSI Savitsky-Golay trend, grey lines: SEVIRI NDVI, dashed grey lines: NDVI 2nd order trend, dotted grey lines: NDVI Savitsky-Golay trend. Field measurements of fresh biomass (g/m^2) shown as solid dots, and vegetation water content (g/m^2) shown as hollow dots.

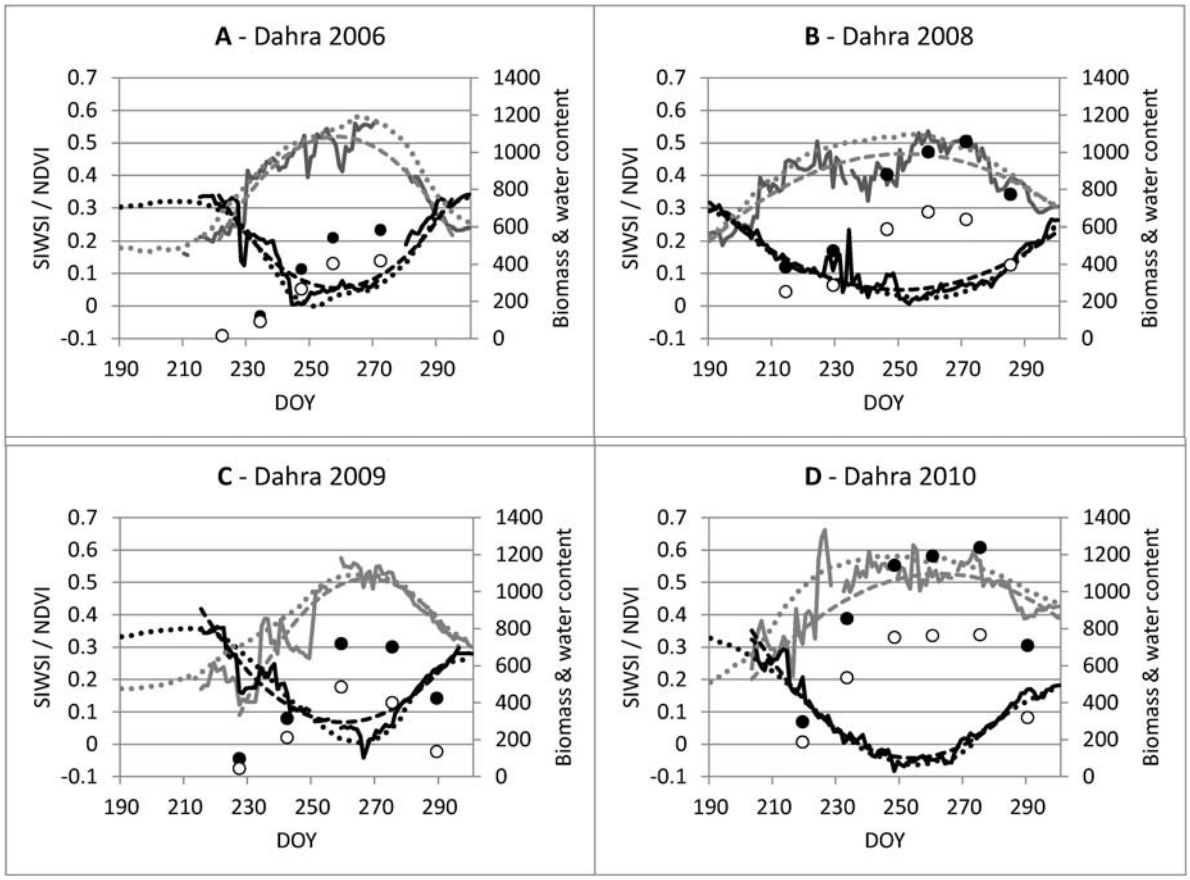

Figure 4. *Cont.*

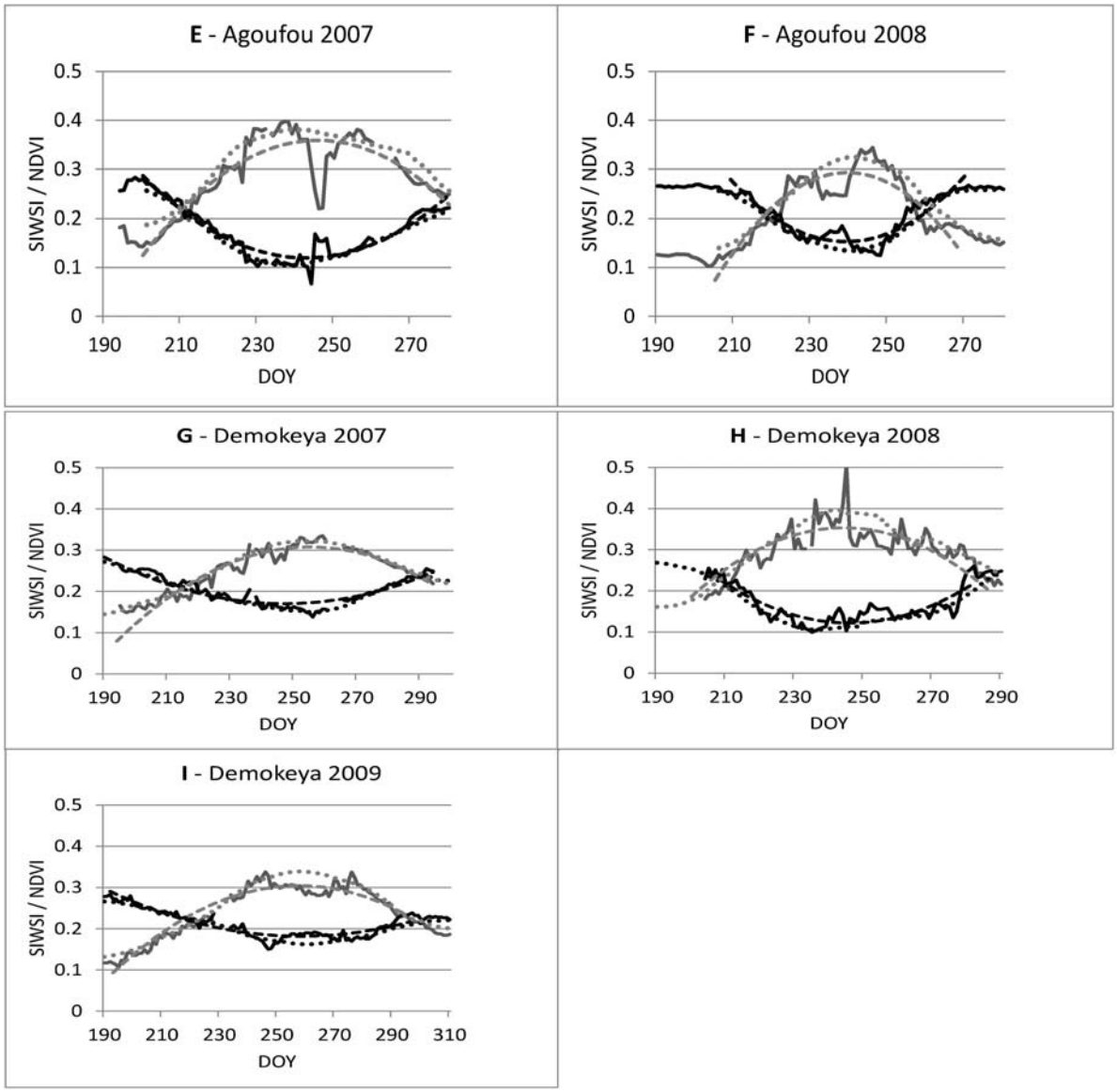

From the Dahra rainfall measurements in Figure 3 and the SMC time series in Figure 5, all the sites have been observed to experience several prolonged periods without significant rainfall in both early, mid- and late-growing seasons. Although it often occurs that SMC is low and insufficient water is available for plant growth, not all years are observed to have these periods of low SMC. In the data presented here the rainfall distribution during the Dahra growing seasons in 2009 and 2010, was such that no periods occurred with insufficient plant available water (Figure 5(A–D)).

For determining periods of low plant water availability a SMC threshold is set to 1% above WP. The periods with low water availability vary in length from two to fourteen days, and are well suited for studying the sensitivity of the anomalies from both indices to plant water stress.

By detrending both the SIWSI and NDVI time series we removed the primary influence of the phenology. SMC and the SIWSI anomalies from detrending with both 2nd order polynomial and Savitsky-Golay are shown in Figure 5, and the NDVI anomalies and SMC are shown in Figure 6. Using 2nd order polynomials for all time series appears to be a valid approach as it fits the satellite based time series quite well despite differences between sites and varying degrees asymmetry of

growing season curves. Using Savitsky-Golay filtering produces trends which are sensitive to intra-seasonal variations in growing season curves, and is able to represent asymmetry. Detrending could be attempted on a shorter time scale using linear trend removal, for, e.g., a week or two of observations, while for full growing seasons some time series might be better described using other functions, but the functions used here fulfilled the need to remove the phenology without removing the short term variations of interest. In the initial data processing it was noticed that using a high order polynomial, e.g., 4th or 5th order, would result in more detailed fits of the function to the respective time series, but the details captured by the higher order polynomials would include some of the short term variation, potential representing the changes that are of interest for comparison with SMC.

Figure 5. Shortwave Infrared Water Stress Index (SIWSI) anomalies and soil moisture: Top pane: SIWSI anomalies from savitsky-golay detrending. Middle pane: SIWSI anomalies from 2nd order detrending (solid dots: SIWSI anomalies during Soil Moisture Content (SMC) < Wilting point (WP) + 1. Hollow dots: SMC > WP + 1). Bottom pane: Dark grey line: SMC. Red line: WP+ 1 (vol.%). Red dashed line: Field capacity (except at Demokeya, here it represents 8 vol.%).

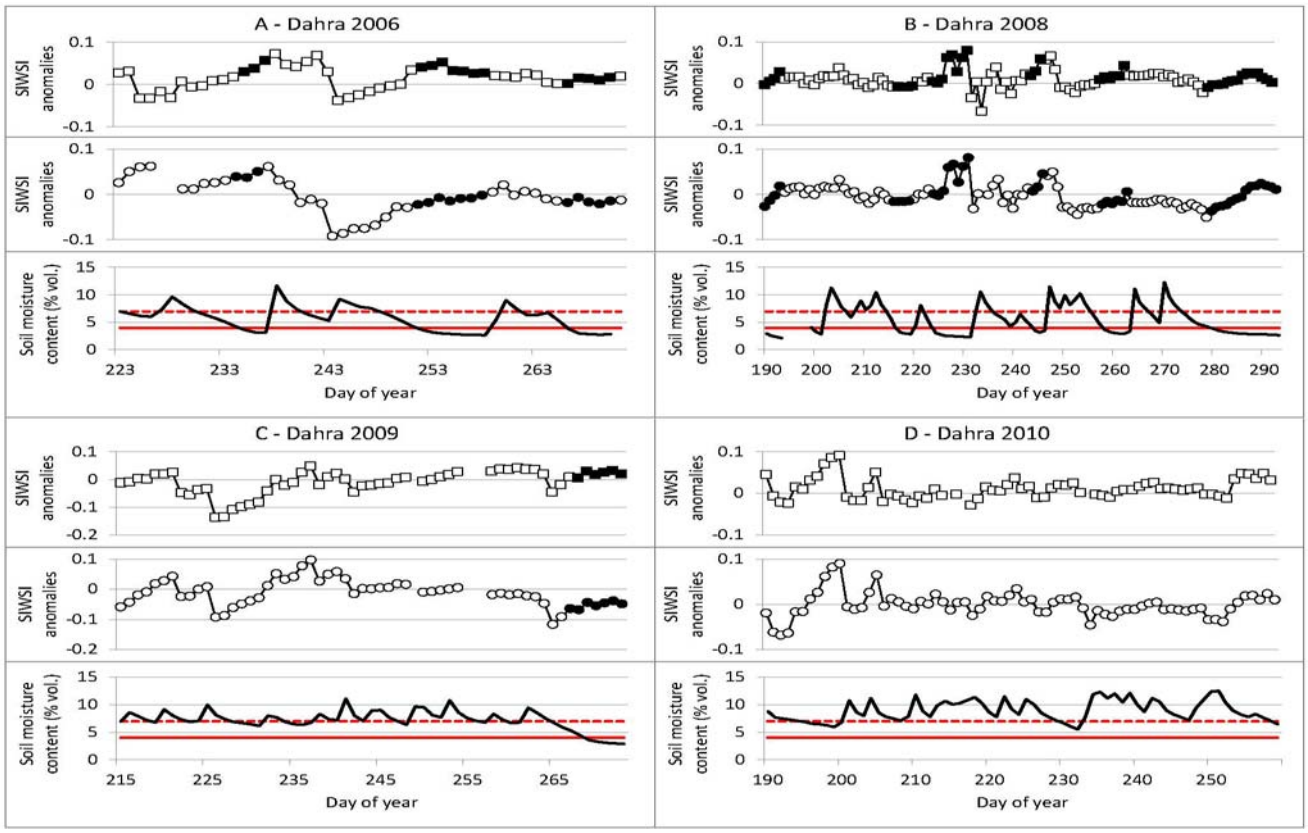

Figure 5. *Cont.*

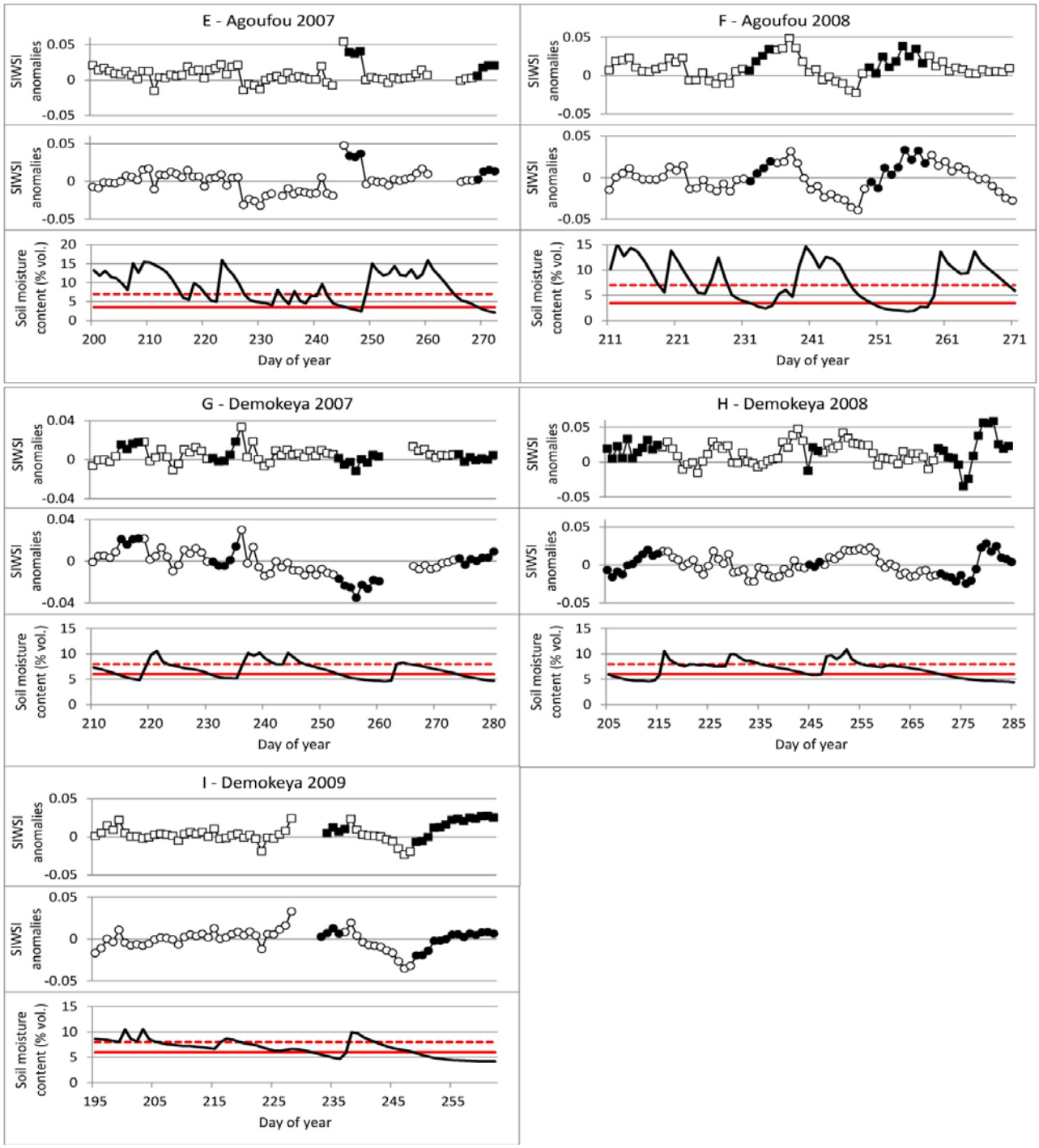

The SIWSI 2nd order anomalies at Dahra are observed to increase when SMC is below WP + 1 (vol.%), with one exception in 2006 (DOY 265 to 269), which is during the late growing season. The Savitsky-Golay anomalies also increase, but have two periods of low SMC where anomalies decrease instead of increasing (DOY 251–257 2006 and DOY 217–220 2008). For many periods both sets of SIWSI anomalies were observed to start increasing already as SMC dropped below Field capacity (FC), and in some cases anomalies increases continuously despite plenty of plant available water having been recorded, as seen several times in the growing seasons of Dahra in 2009 and Demokeya in 2008. For comparison, no systematic relationship between NDVI anomalies, from either of the detrending

methods, and periods of SMC below field capacity was observed at Dahra. At Agoufou only four dry periods of more than two days length were available, and one of these a senescence period in 2007. Both sets of SIWSI anomalies, during the two 2008 dry periods, increase continuously with the number of dry days. The anomalies from Agoufou also appear to start increasing before SMC drops below Wilting point (WP) + 1. Furthermore Agoufou in 2008 is the only site where NDVI anomalies consistently decrease after SMC drops below WP + 1, or FC. At Demokeya neither SIWSI nor NDVI anomalies are observed to increase/decrease consistently when SMC is low.

Figure 6. Normalized Difference Vegetation Index (NDVI) anomalies and soil moisture: Top pane: NDVI anomalies from Savitsky-Golay detrending. Middle pane: NDVI anomalies from 2nd order detrending (solid dots: NDVI anomalies during Soil Moisture Content (SMC) < Wilting point (WP) + 1. Hollow dots: SMC > WP + 1). Bottom pane: Dark grey line: SMC. Red line: WP + 1 (vol.%). Red dashed line: Field capacity (except at Demokeya, here it represents 8 vol.%).

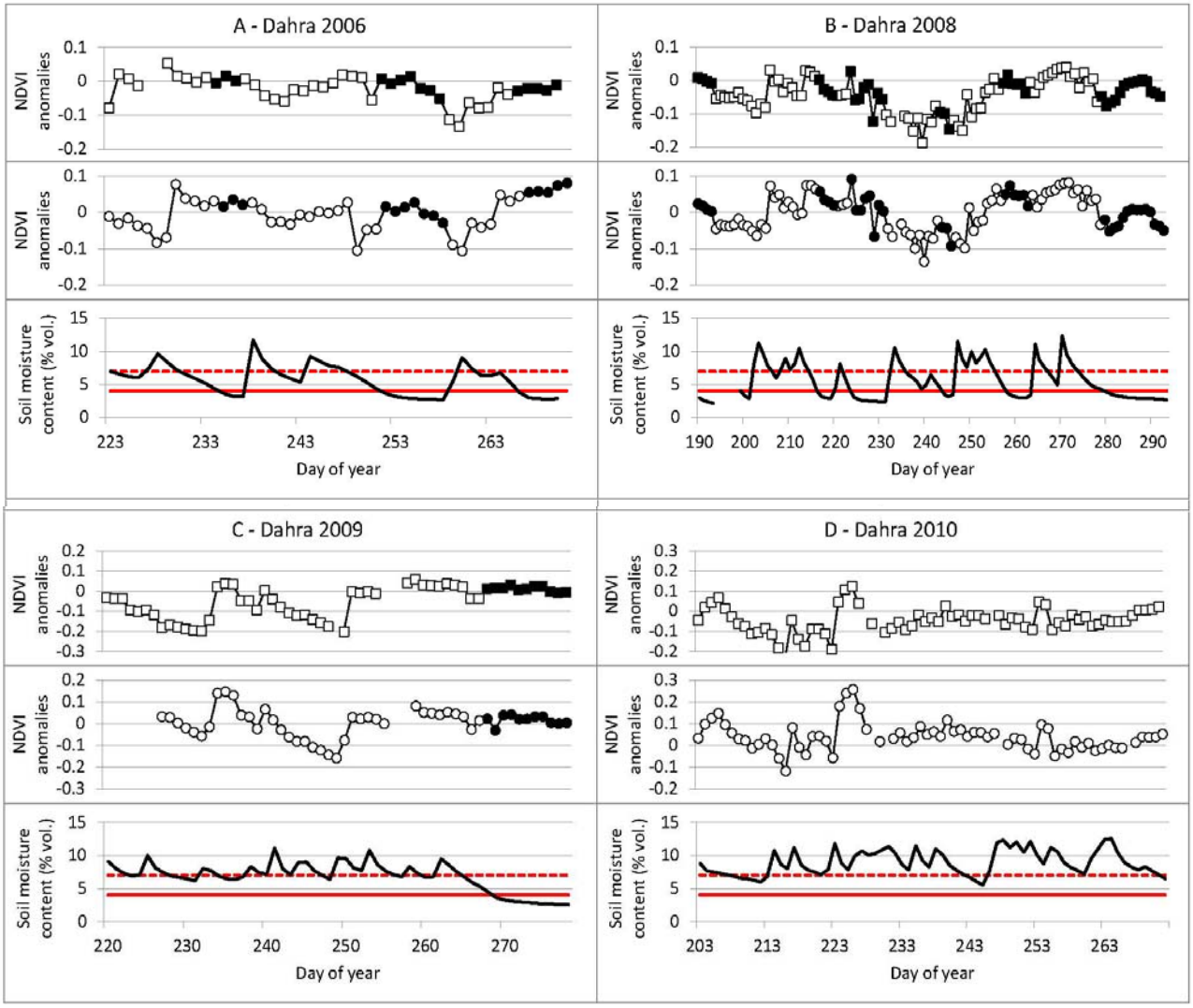

Figure 6. *Cont.*

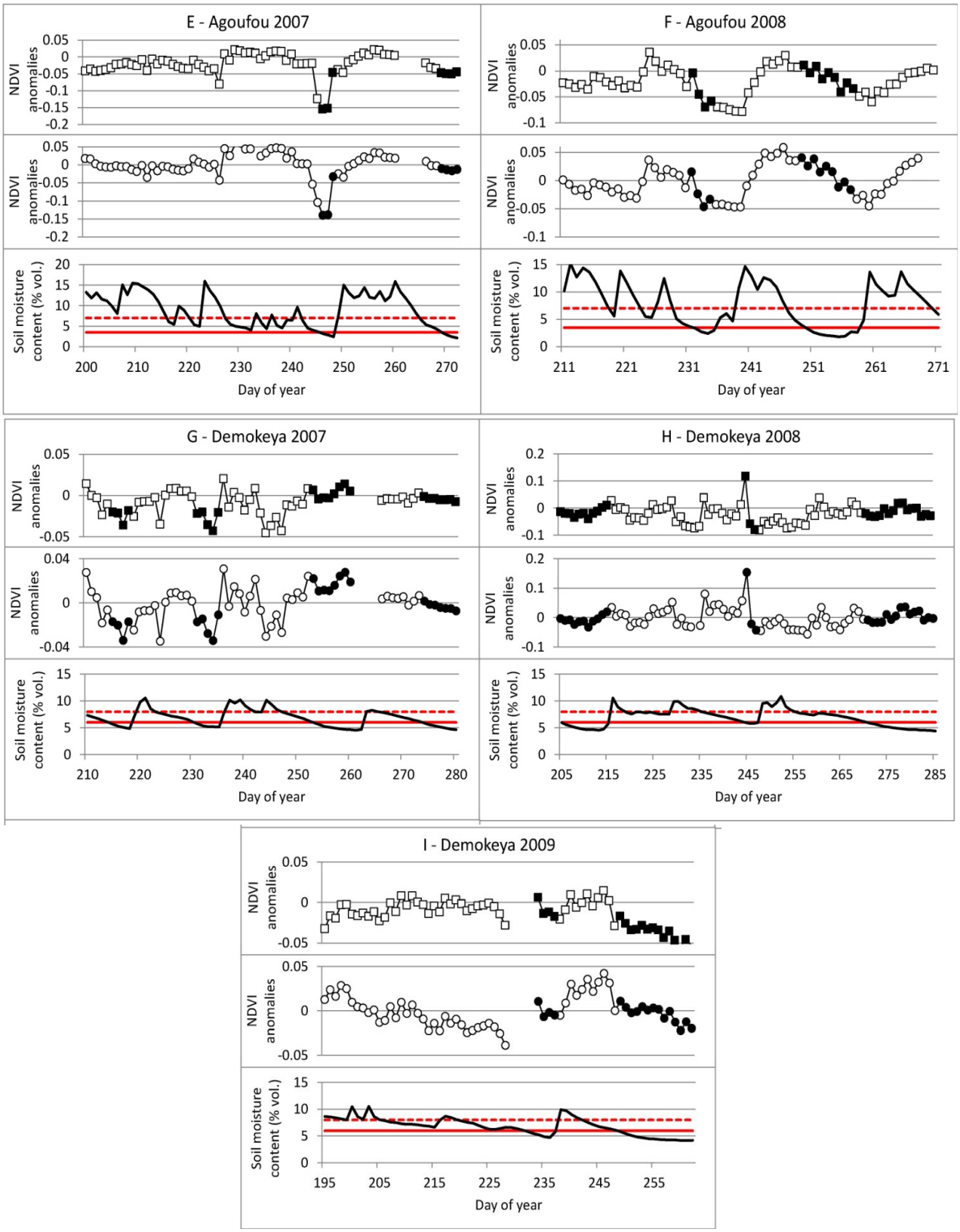

The relationship between number of days with limited plant available water, and the SIWSI and NDVI anomalies, has been examined. For each event lasting three or more days correlation coefficients (r) have been calculated between anomalies and the day numbers after SMC dropped below the threshold of either FC or WP + 1, to assess if anomaly decrease/increase is continuous while SMC is low. From

the number of days and correlations, p-Values have been calculated to indicate statistical significance for the individual events. If using WP + 1 (vol.%) as threshold, correlations are generally higher, while significance is higher for FC threshold, due to the extra number of days designated as dry.

An overview by event and site is shown in Table 5 for SIWSI anomalies and Table 6 for NDVI anomalies and a summary of the number of events with $p < 0.05$, out of the total number of events observed from *in situ* SMC data, is shown in Table 7 for the two sets of anomalies. This shows that the increase in SIWSI anomalies are significant for many periods of plant available water below FC at the Dahra and Agoufou sites, while the periods of SMC < WP + 1 might have high correlations, but are too short to determine whether or not they are statistically significant on $p < 0.05$ level. For the Demokeya site, there is less consistent relationship between increasing SIWSI anomalies, or decreasing NDVI anomalies, and periods of SMC < FC or SMC < WP + 1, although the Savitsky-Golay detrended SIWSI are slightly higher correlated to the dry periods, than the 2nd order detrended SIWSI. It is only for the Agoufou site that NDVI anomalies are found to have significant relationship with all periods of SMC < FC and for anomalies from both detrending methods. For the lower threshold of SMC < WP + 1, there is only a significant relationship for the last long dry period in 2008. Looking at all three sites, the relationships that are significant in most cases, are between anomalies from Savitsky-Golay filtering and periods with SMC < FC for both SIWSI and NDVI, where SIWSI anomalies reflects 19/28 dry events, and NDVI 12/28 events.

Table 5. Overview of Shortwave Infrared Water Stress Index (SIWSI) anomalies and events when low plant available water was observed. Correlation coefficients (r) between number of days after Soil Moisture Content (SMC) dropped below threshold, either Wilting point (WP) + 1 or Field Capacity (FC) (vol.%), and SIWSI anomalies are noted, and p-Values have been calculated based on r and duration in days and marked with Y if $p < 0.05$. Only events of at least three days duration are included.

SIWSI		Field Capacity						Wilting Point + 1					
				2nd Poly.		Savitsky-Golay				2nd Poly.		Savitsky-Golay	
Site	Year	Start DOY	Duration	r	P < 0.05	r	P < 0.05	Start DOY	Duration	r	P < 0.05	r	P < 0.05
Dahra	2006	230	7	0.96	Y	0.98	Y	234	3	0.99	Y	0.97	
Dahra	2006	247	12	0.93	Y	0.49		251	7	0.87	Y	−0.78	
Dahra	2006	261	9	−0.56		−0.24		265	5	−0.29		0.65	
Dahra	2008	190	4	0.99	Y	0.97	Y	190	4	0.99	Y	0.97	Y
Dahra	2008	215	18	0.78	Y	0.84	Y	217	4	0.80		−0.63	
Dahra	2008							224	8	0.83	Y	0.81	Y
Dahra	2008	236	11	0.27		0.39		244	3	0.96		0.87	
Dahra	2008	256	8	0.84	Y	0.90	Y	258	6	0.77	Y	0.80	
Dahra	2008	274	20	0.87	Y	0.52	Y	280	14	0.92	Y	0.63	Y
Dahra	2009	227	4	0.97	Y	0.96	Y	-					
Dahra	2009	233	4	0.57		0.57		-					
Dahra	2009	264	15	0.84	Y	0.79	Y	268	11	0.89	Y	0.79	Y
Dahra	2010	207	6	0.98	Y	0.96	Y	-					
Dahra	2010	242	3	0.81		0.74		-					
Agoufou	2007	227	22	0.64	Y	0.76	Y	246	3	0.68		0.42	
Agoufou	2007	266	7	0.91	Y	0.95	Y	269	4	0.78		0.88	

Table 5. *Cont.*

SIWSI		Field Capacity						Wilting Point + 1					
				2nd Poly.		Savitsky-Golay				2nd Poly.		Savitsky-Golay	
Site	Year	Start DOY	Duration	r	P < 0.05	r	P < 0.05	Start DOY	Duration	r	P < 0.05	r	P < 0.05
Agoufou	2008	229	10	0.96	Y	0.97	Y	232	4	0.99	Y	0.99	Y
Agoufou	2008	247	13	0.9	Y	0.81	Y	250	9	0.80	Y	0.57	
Demokeya	2007	195	8	0.86	Y	0.77	Y	-					
Demokeya	2007	208	12	0.63	Y	0.65	Y	215	4	0.35		0.51	
Demokeya	2007	223	14	0.38		0.53	Y	231	5	0.72		0.78	
Demokeya	2007	247	16	−0.68		−0.38		253	8	0.10		0.00	
Demokeya	2007	266	15	0.82	Y	−0.74		274	7	0.71	Y	0.04	
Demokeya	2008	204	12	0.31		0.55	Y	205	11	0.31		0.36	
Demokeya	2008	219	10	0.54		0.68	Y	-					
Demokeya	2008	235	13	0.57	Y	0.44		245	3	0.80		0.79	
Demokeya	2008	255	32	−0.25		0.26		271	14	0.74	Y	0.48	Y
Demokeya	2009	220	13	0.25		0.53	Y	232	4	0.29		0.45	
Demokeya	2009	242	21	0.76	Y	0.84	Y	249	14	0.96	Y	0.91	Y

Table 6. Overview of Normalized Difference Vegetation Index (NDVI) anomalies and events when low plant available water was observed. Correlation coefficients (r) between number of days after Soil Moisture Content (SMC) dropped below Wilting point (WP) + 1 or Field capacity (FC) (vol.%) and NDVI anomalies are noted, and p-Values have been calculated based on r and duration in days and marked with Y if $p < 0.05$. Only events of at least three days duration are included.

NDVI		Field Capacity						Wilting Point +1					
				2nd Poly.		Savitsky-Golay				2nd Poly.		Savitsky-Golay	
Site	Year	Start DOY	Duration	r	P < 0.05	r	P < 0.05	Start DOY	Duration	r	P < 0.05	r	P < 0.05
Dahra	2006	230	7	0.3		−0.30		234	3	0.00		−0.27	
Dahra	2006	247	12	0.17		−0.64	Y	251	7	−0.81	Y	−0.81	Y
Dahra	2006	261	9	0.82	Y	0.79		265	5	0.89		0.70	
Dahra	2008	190	4	−0.99	Y	−0.98	Y	190	4	−0.99	Y	−0.98	Y
Dahra	2008	215	18	0.54	Y	−0.63	Y	217	4	−0.97	Y	−0.98	Y
Dahra	2008							224	8	−0.49		−0.45	
Dahra	2008	236	11	0.19		0.17		244	3	−0.89		−0.89	
Dahra	2008	256	8	−0.5		−0.45		258	6	−0.73	Y	−0.70	
Dahra	2008	274	20	−0.53	Y	−0.16		280	14	0.11		0.48	
Dahra	2009	227	4	−1	Y	0.99		-					
Dahra	2009	233	4	−0.82		0.84		-					
Dahra	2009	264	15	−0.02		0.02		268	11	−0.17		−0.50	
Dahra	2010	207	6	−0.54		−0.96	Y	-					
Dahra	2010	242	3	−0.84		−0.09		-					
Agoufou	2007	227	22	−0.76	Y	−0.70	Y	246	3	0.87		0.88	
Agoufou	2007	266	7	−0.9	Y	−0.95	Y	269	4	0.48		0.36	
Agoufou	2008	229	10	−0.83	Y	−0.91	Y	232	4	−0.64		−0.85	
Agoufou	2008	247	13	−0.93	Y	−0.92	Y	250	9	−0.92	Y	−0.86	Y
Demokeya	2007	195	8	−0.91	Y	−0.62		-					

Table 6. *Cont.*

NDVI		Field Capacity						Wilting Point +1					
				2nd Poly.		Savitsky-Golay				2nd Poly.		Savitsky-Golay	
Site	Year	Start DOY	Duration	r	P < 0.05	r	P < 0.05	Start DOY	Duration	r	P < 0.05	r	P < 0.05
Demokeya	2007	208	12	−0.9		−0.84		215	4	−0.22		−0.14	
Demokeya	2007	223	14	0.03		−0.22		231	5	−0.11		−0.31	
Demokeya	2007	247	16	0.72		0.70	Y	253	8	0.48		0.55	
Demokeya	2007	266	15	−0.85	Y	−0.08		274	7	−0.97	Y	−0.93	Y
Demokeya	2008	204	12	0.44		0.47		205	11	0.44		0.52	
Demokeya	2008	219	10	0.7		0.59		-					
Demokeya	2008	235	13	0.41		0.00		245	3	0.00		−0.91	
Demokeya	2008	255	32	0.63		0.29		271	14	0.48		−0.06	
Demokeya	2009	220	13	0.63		−0.26		232	4	−0.69		−0.85	
Demokeya	2009	242	21	−0.88	Y	−0.91	Y	249	14	−0.84	Y	−0.90	Y

Table 7. Number of dry events, out of total number of dry events, where Shortwave Infrared Water Stress Index (SIWSI) anomalies are increasing, or Normalized Difference Vegetation Index (NDVI) anomalies are decreasing, significantly ($p < 0.05$) in comparison with number of days after Soil Moisture Content (SMC) drops below threshold. Wilting point (WP) + 1 and Field capacity (FC) are both tested as thresholds. Anomalies are derived using both 2nd order polynomials and Savitsky-Golay smoothing.

Site	SIWSI Detrended Using 2nd Order Polynomial		SIWSI Detrended Using Savitsky-Golay Smoothing		NDVI Detrended Using 2nd Order Polynomial		NDVI Detrended Using Savitsky-Golay Smoothing	
	FC	WP + 1	FC	WP + 1	FC	WP + 1	FC	WP + 1
Dahra	9/13	7/10	8/13	4/10	5/13	3/10	4/13	4/9
Agoufou	4/4	2/4	4/4	1/4	4/4	1/4	4/4	1/4
Demokeya	5/11	2/9	7/11	1/9	2/11	2/9	4/11	3/9
Total	18/28	11/23	19/28	6/23	11/28	6/23	12/28	8/23

7. Discussion

7.1. Land Surface Moisture during Period of Bare Soil

For detection of soil moisture variations using satellite remote sensing, the *in situ* data provide valuable insights of the temporal variability of soil moisture and the possibility to detect changes using soil reflectances. Although a darkening of the soil is clearly observable from *in situ* data following rainfall, the short time scale, and the lack of data in the VNIR and SWIR spectrums during night time, pose challenges even for high temporal resolution products, such as the daily NBAR product produced using the geostationary MSG SEVIRI data. In our case study, based on sandy soil, it is difficult to detect any changes in soil reflectance and soil moisture using satellite data with a daily or lower temporal resolution. This is of particular importance for certain applications such as monitoring soil moisture in desert regions for identifying areas favorable for Desert Locust breeding [59].

The *in situ* measurements of land surface temperature suggest that a thermal product using a diurnal variation range with data available on an hourly basis will have a better potential for detecting changes in bare soil SMC. The presence of evaporable water in the soil still acts as a dampener on the temperature range a few hours after the visible and short wave surface reflectances have returned to the dry state. The *in situ* daily averaged NDVI values calculated for the two bare soil case periods are not seen to change much as a result of the rainfall events, but the following initiation of germination and greening causes NDVI to increase shortly after, as seen in the 2006 case. The short lag between first rainfalls and increasing NDVI compares well to climate room tests made by [60] concerning the germination rates of annual plant species common in the Sahel. They showed that for several species, up to 75% of viable seeds germinated within one or two days. This means that although studies have investigated the effect of different soil and soil brightness backgrounds for canopy reflectances, e.g., [25], variations observed for mixed soil/canopy reflectances are less likely to reflect changes in soil brightness, caused by SMC changes, and more likely to be caused by longer term changes, specifically plant growth. Results from a study using simulated data by [61] suggest that combining NIR-SWIR data into normalized indices reduces the sensitivity to variations in soil brightness as compared to the respective spectral intervals alone. Therefore, when using processed satellite based red/NIR or NIR/SWIR observations to calculate normalized indices on a daily basis, the effects of SMC variations can be expected to be even smaller, and the SEVIRI NDVI and SEVIRI SIWSI time series should be largely unaffected by short variations in soil moisture as the ones observed in the sandy soil of Dahra, Agoufou and Demokeya.

7.2. Land Surface Moisture during Period of Vegetation Growth

While both NDVI and SIWSI followed vegetation phenology, the inter-annual differences in relationship found between SIWSI, biomass and water content is puzzling. Previous sensitivity analyses have found the NIR spectrum to be more sensitive to leaf internal structure than to leaf dry matter content [30], and as the observations are from an area of natural vegetation with relatively low biomass production, and where year-to-year variations in annual species composition occur, changes in dominant species can be part of the explanation. This is further supported by the *in situ* NDVI time series, where no straight forward relation between NDVI, either the maximum or the seasonal integral, is observed as compared to biomass e.g., the maximum NDVI values were observed on the year of lowest biomass production (2006), but the four years of data are insufficient for conclusions. Previous study using *in situ* data in a semi-arid environment has shown high temporal resolution NDVI to be able to distinguish between the same species exposed to different growing conditions, but for sites where the vegetation is dominated by the perennial *Sarcobatus vermiculatus* (greasewood) [62]. Therefore study into the extent that natural variation in species composition affects satellite based vegetation water indices and vegetation greenness indices, would provide some important perspectives for interpreting these indices for the Sahel.

Although the time series of NDVI and SIWSI appears closely interrelated during growing seasons, some differences become obvious when examining the anomalies after detrending, as the increase in SIWSI anomalies during dry periods are significant more often than the decrease in NDVI anomalies. The difference in anomalies depending on the detrending method does not appear to have a big impact, but the combination which results in significant relationships for most events is Savitsky-Golay

detrended SIWSI *vs.* the number of days after SMC drops below FC, with one event more than the 2nd order detrended SIWSI. The reason for the less systematic relationship between SIWSI anomalies and low SMC at the Demokeya site is not easy to answer with the data presented here, but compared to Agoufou and Dahra, the Demokeya site is geographically far removed.

From the comparison between anomalies, SMC and the two thresholds (FC and WP+1), we can see many periods are observed where SIWSI anomalies increase already when SMC drops below field capacity, and sometimes even before that. This indicates that identifying periods of SMC close to wilting point from increases in detrended SIWSI time series is not straight forward, and anomalies cannot be expected to reflect a fixed SMC threshold. While assuming SIWSI anomalies increase when there is little plant available water seems to have some validity, the anomalies from both detrending methods are sometimes found to increase when records show that plenty of water is available. This, together with a noticeable number of dry periods where SIWSI anomalies do not increase during dry periods, makes it unlikely that detrended vegetation water indices can be implemented for reliable water stress detection. With inter-annual variation in plant species composition and as species differ in drought resilience and response to water stress, the complex vegetation dynamics of the Sahel, together with the low spatial resolution of geostationary images and inherent noise in satellite data, can be part of the explanation as to why the detrended SIWSI does not react in a more consistent way to low levels of SMC.

As the use of SWIR based vegetation water indices in the early growing season are considered especially challenging, due to sparse vegetation cover, four dry events during the early growing seasons at Dahra are of interest; the first in 2006 and the three first in 2008. They can be classified as early growing season from a combination of low biomass and still increasing *in situ* NDVI. During these four periods the 2nd order SIWSI anomalies all have high correlation with the number of days of SMC < WP + 1 and three of the four periods are found significant ($p < 0.05$). For Savitsky-Golay SIWSI anomalies, the correlations are lower and only two events have significant relationship. Although four cases are insufficient for conclusions, it indicates that the SIWSI anomalies are at least somewhat sensitive to dry periods in the early growing seasons. In the other end of a growing season, during senescence when annual plants are dying, analyzing anomalies for water stress detection is less meaningful, but for fire risk assessment a recent study did find consistent significant relationships between several NIR/SWIR based indices and herbaceous water content during senescence, concluding that remote sensing is a powerful tool for monitoring the drying process of herbaceous vegetation [63].

Studies into detrending vegetation water indices for other regions where water stress are common could be interesting. This could reveal if the method is more robust for areas with, e.g., more dense vegetation cover than the sites examined here.

8. Conclusions

From the combined use of Spinning Enhanced Visible and Near Infrared Imager (SEVIRI) and *in situ* observations, we have addressed the potential of geostationary satellite observations for estimating surface moisture during bare soil conditions, and the challenge of deriving information on variations in water status from the Shortwave Infrared Water Stress Index (SIWSI), during the early to mid- growing season in semi arid Sahel.

Rainfall events during bare soil conditions resulted in a noticeable decrease in *in situ* red and Near Infrared (NIR) reflectance of 50%~70%, but this decrease is only observable on a very short sub-diurnal time scale. This makes the daily Nadir View BRDF Adjusted Reflectance (NBAR) product produced using four days of observations from the SEVIRI instrument, unlikely to be sensitive to rainfall induced variations in soil brightness, even when there is no or little vegetation. Therefore, despite the high temporal resolution as compared to other satellite products, the sensitivity of the geostationary satellite based Normalized Difference Vegetation Index (NDVI) and SIWSI to variations in soil brightness is limited, even before much vegetation cover is present. Also during bare soil conditions, a decrease in diurnal range of Land Surface Temperature (LST) from 30 °C to 10 °C was observed following the first rainfall events. Therefore we propose that future research is conducted to monitor rapid decrease in soil surface temperature for estimation of rainfall events and presence of wet soil, using LST from the SEVIRI sensor at high temporal resolution (measurements at least every hour) independently of the time of the rain event (night or day).

We investigated a simple method for assessing short term changes in vegetation water status, by detrending seasonal dependent time series of vegetation water sensitive indices. For the NBAR product applied in this study the trend removal from time series of SIWSI results in anomalies, which increase continuously during periods where little plant available water is present. In comparison NDVI anomalies were observed to decrease, but far less systematically.

Anomalies from index detrending using 2nd order polynomials and Savitsky-Golay filtering was compared with number of days after Soil Moisture Content (SMC) dropped below thresholds of Field Capacity (FC) or Wilting Point + 1 vol.% (WP+1). For both SIWSI and NDVI the increase/decrease of anomalies was found statistically significant for the most cases ($p < 0.05$) when detrending was performed using Savitsky-Golay filtering and anomalies were related to number of days when SMC was below FC, with respectively 19 out of 28 dry periods for SIWSI anomalies and 12 out of 28 dry periods for NDVI anomalies.

While SIWSI may carry complementary information to NDVI in terms of vegetation water status, the relationship between increasing SIWSI anomalies and dry periods does not appear to be very robust, and the anomalies often increase when there is abundant plant available water. Therefore, while the study confirms near- and shortwave infrared based vegetation water indices as being useful surface moisture indicators, the method of detrending time series of geostationary shortwave infrared data for water stress detection in the Sahel is not recommended in its present state. Further studies into detrending on shorter timescales and in combination with thermal data could be interesting, as well as investigation of sub-pixel variations in SMC for the more heterogeneous areas of the Sahel.

Conflicts of Interest

The author declares no conflict of interest.

References

1. Eagleson, P.S. Ecological optimality in water-limited natural soil-vegetation systems. 1. Theory and hypothesis. *Water Resour. Res.* **1982**, *18*, 325–340.

2. Rodriguez-Iturbe, I.; Porporato, A. *Ecohydrology of Water-Controlled Ecosystems, Soil Moisture and Plant Dynamics*; Cambridge University Press: Cambridge, UK, 2004.
3. Koster, R.D.; Dirmeyer, P.A.; Guo, Z.C.; Bonan, G.; Chan, E.; Cox, P.; Gordon, C.T.; Kanae, S.; Kowalczyk, E.; Lawrence, D.; *et al*. Regions of strong coupling between soil moisture and precipitation. *Science* **2004**, *305*, 1138–1140.
4. Hutchinson, C.F. Uses of satellite data for famine early warning in Sub-Saharan Africa. *Int. J. Remote Sens.* **1991**, *12*, 1405–1421.
5. Thornton, P.K.; Bowen, W.T.; Ravelo, A.C.; Wilkens, P.W.; Farmer, G.; Brock, J.; Brink, J.E. Estimating millet production for famine early warning: An application of crop simulation modelling using satellite and ground-based data in Burkina Faso. *Agric. For. Meteorol.* **1997**, *83*, 95–112.
6. Anyamba, A.; Tucker, C.J.; Huete, A.R.; Boken, V.K. Monitoring Drought Using Coarse-Resolution Polar-Orbiting Satellite Data. In *Monitoring and Predicting Agricultural Drought: A Global Study*; Boken, V.K., Cracknell, A.P., Heathcote, R.L., Eds.; Oxford Univerisity Press: New York, NY, USA, 2005.
7. Kerr, Y.H.; Waldteufel, P.; Wigneron, J.P.; Delwart, S.; Cabot, F.; Boutin, J.; Escorihuela, M.J.; Font, J.; Reul, N.; Gruhier, C.; *et al*. The SMOS Mission: New tool for monitoring key elements of the global water cycle. *Proc. IEEE* **2010**, *98*, 666–687.
8. Carlson, T.N.; Ripley, D.A. A method to make use of thermal infrared temperature and NDVI measurements to infer surface soil water content and fractional vegetation cover. *Remote Sens. Rev.* **1994**, *9*, 161–173.
9. Gillies, R.R.; Carlson, T.N.; Cui, J.; Kustas, W.P.; Humes, K.S. A verification of the "triangle" method for obtaining surface soil water content and energy fluxes from remote measurements of the Normalized Difference Vegetation Index (NDVI) and surface radiant temperature. *Int. J. Remote Sens.* **1997**, *18*, 3145–3166.
10. Sandholt, I.; Rasmussen, K.; Andersen, J. A simple interpretation of the surface temperature/vegetation index space for assessment of surface moisture status. *Remote Sens. Environ.* **2002**, *79*, 213–224.
11. Krapez, J.C.; Olioso, A. A combination of temperature, vegetation indexes and albedo, as obtained by airborne hyperspectral remote sensing, for the evaluation of soil moisture. *QIRT J.* **2011**, *8*, 187–200.
12. Loomis, W.E. Absorption of radiant energy by leaves. *Ecology* **1965**, *46*, 14–24.
13. Olson, C.E. Accuracy of land-use interpretation from infrared imagery in the 4.5 to 5.5 micron band. *Ann. Assoc. Am. Geogr.* **1967**, *57*, 382–388.
14. Tucker, C.J. Remote-sensing of leaf water-content in the near-infrared. *Remote Sens. Environ.* **1980**, *10*, 23–32.
15. Gao, B.-C.; Goetz, A.F.H. Retrieval of equivalent water thickness and information related to biochemical-components of vegetation canopies from aviris data. *Remote Sens. Environ.* **1995**, *52*, 155–162.
16. Gao, B.-C. NDWI—A normalized difference water index for remote sensing of vegetation liquid water from space. *Remote Sens. Environ.* **1996**, *58*, 257–266.

17. Moran, M.S.; Clarke, T.R.; Inoue, Y.; Vidal, A. Estimating crop water-deficit using the relation between surface-air temperature and spectral vegetation index. *Remote Sens. Environ.* **1994**, *49*, 246–263.
18. Goetz, S.J. Multi-sensor analysis of NDVI, surface temperature and biophysical variables at a mixed grassland site. *Int. J. Remote Sens.* **1997**, *18*, 71–94.
19. Stisen, S.; Sandholt, I.; Norgaard, A.; Fensholt, R.; Jensen, K.H. Combining the triangle method with thermal inertia to estimate regional evapotranspiration—Applied to MSG-SEVIRI data in the Senegal River basin. *Remote Sens. Environ.* **2008**, *112*, 1242–1255.
20. Tucker, C.J. Red and photographic infrared linear combinations for monitoring vegetation. *Remote Sens. Environ.* **1979**, *8*, 127–150.
21. Carlson, T.N.; Ripley, D.A. On the relation between NDVI, fractional vegetation cover, and leaf area index. *Remote Sens. Environ.* **1997**, *62*, 241–252.
22. Daughtry, C.S.T. Discriminating crop residues from soil by shortwave infrared reflectance. *Agron. J.* **2001**, *93*, 125–131.
23. Tucker, C.J. Comparison of satellite sensor bands for vegetation monitoring. *Photogramm. Eng. Remote Sensing* **1978**, *44*, 1369–1380.
24. Ben-Dor, E.; Irons, J.R.; Epeman, G.F. Soil Reflectance. In *Manual of Remote Sensing: Remote Sensing for the Earth Sciences*, 3rd ed.; Wiley & Sons: New York, NY, USA, 1999; pp. 111–173.
25. Huete, A.R.; Jackson, R.D.; Post, D.F. Spectral response of a plant canopy with different soil backgrounds. *Remote Sens. Environ.* **1985**, *17*, 37–53.
26. Lobell, D.B.; Asner, G.P. Moisture effects on soil reflectance. *Soil Sci. Soc. Amer. J.* **2002**, *66*, 722–727.
27. Small, C.; Steckler, M.; Seeber, L.; Akhter, S. H.; Goodbred, S.; Mia, B.; Imam, B. Spectroscopy of sediments in the Ganges-Brahmaputra delta: Spectral effects of moisture, grain size and lithology. *Remote Sens. Environ.* **2009**, *113*, 342–361.
28. Samain, O.; Kergoat, L.; Hiernaux, P.; Guichard, F.; Mougin, E.; Timouk, F.; Lavenu, F. Analysis of the *in situ* and MODIS albedo variability at multiple timescales in the Sahel. *J. Geophys. Res. Atmos.* **2008**, doi: 10.1029/2007JD009174.
29. Ceccato, P.; Flasse, S.; Tarantola, S.; Jacquemoud, S.; Gregoire, J.M. Detecting vegetation leaf water content using reflectance in the optical domain. *Remote Sens. Environ.* **2001**, *77*, 22–33.
30. Ceccato, P.; Gobron, N.; Flasse, S.; Pinty, B.; Tarantola, S. Designing a spectral index to estimate vegetation water content from remote sensing data—Part 1. Theoretical approach. *Remote Sens. Environ.* **2002**, *82*, 188–197.
31. Ceccato, P.; Flasse, S.; Gregoire, J.M. Designing a spectral index to estimate vegetation water content from remote sensing data—Part 2. Validation and applications. *Remote Sens. Environ.* **2002**, *82*, 198–207.
32. Fensholt, R.; Sandholt, I. Derivation of a shortwave infrared water stress index from MODIS near- and shortwave infrared data in a semiarid environment. *Remote Sens. Environ.* **2003**, *87*, 111–121.
33. Sjöstrom, M.; Ardo, J.; Eklundh, L.; El-Tahir, B.A.; El-Khidir, H.A.M.; Hellstrom, M.; Pilesjo, P.; Seaquist, J. Evaluation of satellite based indices for gross primary production estimates in a sparse savanna in the Sudan. *Biogeosciences* **2009**, *6*, 129–138.

34. Fensholt, R.; Huber, S.; Proud, S.R.; Mbow, C. Detecting canopy water status using shortwave infrared reflectance data from polar orbiting and geostationary platforms. *IEEE J. Sel. Top. Appl. Earth Obs. Remote Sens.* **2010**, *3*, 271–285.
35. Love, T. *The Climate Prediction Center Rainfall Estimation Algorithm Version 2*; Climate Prediction Center-National Oceanic and Atmospheric Association (NOAA): College Park, MD, USA, 2002.
36. Food and Agriculture Organization of the United Nations (FAO-UN)/International Union of Soil Sciences (IUSS) Working Group. *World Reference Base for Soil Resources 2006—A Framework for International Classification, Correlation and Communication*; FAO-UN: Rome, Italy, 2006; Volume 103.
37. Food and Agriculture Organization (FAO). *Harmonized World Soil Database (version 1.1)*; FAO: Rome, Italy, 2009.
38. Fensholt, R.; Sandholt, I.; Stisen, S. Evaluating MODIS, MERIS, and VEGETATION—Vegetation indices using *in situ* measurements in a semiarid environment. *IEEE Trans. Geosci. Remote Sens.* **2006**, *44*, 1774–1786.
39. Proud, S.R.; Rasmussen, M.O.; Fensholt, R.; Sandholt, I.; Shisanya, C.; Mutero, W.; Mbow, C.; Anyamba, A. Improving the SMAC atmospheric correction code by analysis of Meteosat Second Generation NDVI and surface reflectance data. *Remote Sens. Environ.* **2010**, *114*, 1687–1698.
40. Rasmussen, M.O.; Gottsche, F.M.; Diop, D.; Mbow, C.; Olesen, F.S.; Fensholt, R.; Sandholt, I. Tree survey and allometric models for tiger bush in northern Senegal and comparison with tree parameters derived from high resolution satellite data. *Int. J. Appl. Earth Obs. Geoinf.* **2011**, *13*, 517–527.
41. Mougin, E.; Hiernaux, P.; Kergoat, L.; Grippa, M.; de Rosnay, P.; Timouk, F.; Le Dantec, V.; Demarez, V.; Lavenu, F.; Arjounin, M.; *et al*. The AMMA-CATCH Gourma observatory site in Mali: Relating climatic variations to changes in vegetation, surface hydrology, fluxes and natural resources. *J. Hydrol.* **2009**, *375*, 14–33.
42. African Monsoon Multi-Disciplinary Analysis (AMMA). Available online: http://www.amma-international.org (accessed on 4 December2012).
43. Hiernaux, P.; Mougin, E.; Diarra, L.; Soumaguel, N.; Lavenu, F.; Tracol, Y.; Diawara, M. Sahelian rangeland response to changes in rainfall over two decades in the Gourma region, Mali. *J. Hydrol.* **2009**, *375*, 114–127.
44. Elberling, B.; Fensholt, R.; Larsen, L.; Petersen, A.-I. S.; Sandholt, I. Water content and land use history controlling soil CO_2 respiration and carbon stock in savanna soil and groundnut fields in semi-arid Senegal. *Geografisk Tidsskrift-Dan. J. Geogr.* **2003**, *103*, 47–56.
45. Ardö, J.; Mölder, M.; El-Tahir, B.A.; Elkhidir, H.A.M. Seasonal variation of carbon fluxes in a sparse savanna in semi arid Sudan. *Carbon Balanc. Manag.* **2008**, doi: 10.1186/1750-0680-3-7.
46. Möllerström, L. Modelling Soil Temperature & Soil Water Availability in Semi-Arid Sudan: Validation and Testing. M.Sc. Thesis, Lund University: Lund, Sweden, 2004.
47. Schmetz, J.; Pili, P.; Tjemkes, S.; Just, D.; Kerkmann, J.; Rota, S.; Ratier, A. An introduction to Meteosat Second Generation (MSG). *Bull. Amer. Meteorol. Soc.* **2002**, *83*, 977–992.

48. Proud, S.R.; Fensholt, R.; Rasmussen, M.O.; Sandholt, I. A comparison of the effectiveness of 6S and SMAC in correcting for atmospheric interference of Meteosat Second Generation images. *J. Geophys. Res.-Atmos.* **2010**, doi: 10.1029/2009JD013693.
49. Rahman, H.; Dedieu, G. Smac—A simplified method for the atmospheric correction of satellite measurements in the solar spectrum. *Int. J. Remote Sens.* **1994**, *15*, 123–143.
50. Lutz, H.J. *Cloud Detection for MSG—Algorithm Theoretical Basis Document (ATBD); EUM/MET/REP/07/0132 v2*; The European Organisation for the Exploitation of Meteorological Satellites (EUMETSAT): Darmstadt, Germany, 14 November 2007; Volume 2.
51. Schaaf, C.B.; Gao, F.; Strahler, A.H.; Lucht, W.; Li, X; Tsang, T.; Strugnell, N.C.; Zhang, X.; Jin, Y.; Muller, J-P.; *et al.* First operational BRDF, albedo nadir reflectance products from MODIS. *Remote Sens. Environ.* **2002**, *83*, 135–148.
52. Proud, S.R.; Zhanf, Q.; Schaaf, C.; Fensholt, R.; Rasmussen, M.O.; Shisanya, C.; Mutero, W.; Mbow, C.; Anyamba, A.; Pak, E.; *et al*. The normalization of the surface anisotropy effects present in SEVIRI reflectance data by using the MODIS BRDF method. *IEEE Trans. Geosci. Remote Sens*. **2013**, in reivew..
53. De Rosnay, P.; Gruhier, C.; Timouk, F.; Baup, F.; Mougin, E.; Hiernaux, P.; Kergoat, L.; LeDantec, V. Multi-scale soil moisture measurements at the Gourma meso-scale site in Mali. *J. Hydrol.* **2009**, *375*, 241–252.
54. Mbow, C.; Fensholt, R.; Rasmussen, K.; Diop, D. Can vegetation productivity be derived from greenness in a semi-arid environment? Evidence from ground based measurements. *J. Arid Environ.* **2013**, in press.
55. Tracol, Y.; Mougin, E.; Hiernaux, P.; Jarlan, L. Testing a sahelian grassland functioning model against herbage mass measurements. *Ecol. Model.* **2006**, *193*, 437–446.
56. Boone, A.; De Rosnay, P.; Balsamo, G.; Beljaars, A.; Chopin, F.; Decharme, B.; Delire, C.; Ducharne, A.; Gascoin, S.; Grippa, M.; *et al*. The amma land surface model intercomparison project (almip). *Bull. Amer. Meteorol. Soc.* **2009**, *90*, 1865–1880.
57. Kaufman, Y.J.; Tanre, D.; Remer, L.A.; Vermote, E.F.; Chu, A.; Holben, B.N. Operational remote sensing of tropospheric aerosol over land from EOS moderate resolution imaging spectroradiometer. *J. Geophys. Res.-Atmos.* **1997**, *102*, 17051–17067.
58. Levy, R.C.; Remer, L.A.; Tanré, D.; Mattoo, S.; Kaufmann, R.K. *Algorithm for Remote Sensing of Tropospheric Aerosol over Dark Targets from MODIS: Collections 005 and 051*; National Aeronautics and Space Administration (NASA): Greenbelt, MD, USA, 2009.
59. Ceccato, P.; Cressman, K.; Giannini, A.; Trzaska, S. The desert locust upsurge in West Africa (2003–2005): Information on the desert locust early warning system and the prospects for seasonal climate forecasting. *Int. J. Pest Manag.* **2007**, *53*, 7–13.
60. Elberse, W.T.; Breman, H. Germination and establishment of sahelian rangeland species—1. Seed properties. *Oecologia* **1989**, *80*, 477–484.
61. Wang, L.L.; Qu, J.J.; Hao, X.J.; Zhu, Q.P. Sensitivity studies of the moisture effects on MODIS SWIR reflectance and vegetation water indices. *Int. J. Remote Sens.* **2008**, *29*, 7065–7075.
62. Baghzouz, M.; Devitt, D.A.; Fenstermaker, L.F.; Young, M.H. Monitoring vegetation phenological cycles in two different semi-arid environmental settings using a ground-based NDVI system: A potential approach to improve satellite data interpretation. *Remote Sens.* **2010**, *2*, 990–1013.

63. Sow, M.; Mbow, C.; Hély, C.; Fensholt, R.; Sambou, B. Estimation of herbaceous fuel moisture content using vegetation indices and land surface temperature from MODIS data. *Remote Sens.* **2013**, *5*, 2617–2638.